Received 2 July 2021; revised 2 August 2021; accepted 21 August 2021. Date of publication 24 August 2021; date of current version 7 September 2021.

Digital Object Identifier 10.1109/OJCOMS.2021.3107287

Massive Measurements of 5G Exposure in a Town: Methodology and Results

LUCA CHIARAVIGLIO [1,2] (Senior Member, IEEE), CHIARA LODOVISI [1,2], DANIELE FRANCI [3], SETTIMIO PAVONCELLO [3], TOMMASO AURELI [3], NICOLA BLEFARI-MELAZZI [1,2], AND MOHAMED-SLIM ALOUINI [4]

[1]Department of Electronic Engineering, University of Rome Tor Vergata, 00133 Rome, Italy

[2]Consorzio Nazionale Interuniversitario per le Telecomunicazioni, 43124 Parma, Italy

[3]Agenzia per la Protezione Ambientale del Lazio, 00173 Rome, Italy

[4]Computer, Electrical, and Mathematical Science and Engineering Division, King Abdullah University of Science and Technology, Thuwal 6900, Makkah, Saudi Arabia

CORRESPONDING AUTHOR: L. CHIARAVIGLIO (e-mail: luca.chiaraviglio@uniroma2.it)

This work was supported by the PLAN-EMF Project (KAUST) under Award OSR-2020-CRG9-4377.

ABSTRACT We target the problem of performing a large set of measurements over the territory to characterize the exposure from a 5G deployment. Since using a single Spectrum Analyzer (SA) is not practically feasible (due to the limited battery duration), in this work we adopt an integrated approach, based on the massive measurement of 5G metrics with a 5G smartphone, followed by a detailed analysis done with the SA and an ElectroMagnetic Field (EMF) meter in selected locations. Results, obtained over a real territory covered by 5G signal, reveal that 5G exposure is overall very limited for most of measurement locations, both in terms of field strength (up to 0.7 [V/m]) and as share w.r.t. other wireless technologies (typically lower than 15%). Moreover, our approach allows easily spotting measurement outliers, e.g., due to the exploitation of Dynamic Spectrum Sharing (DSS) techniques between 4G and 5G. In addition, the exposure metrics collected with the smartphone are overall a good proxy of the total exposure measured over the whole 5G channel. Moreover, the sight conditions and the distance from 5G base station play a great role in determining the level of exposure. Finally, a maximum of 130 [W] of power radiated by a 5G base station is estimated in the scenario under consideration.

INDEX TERMS 5G cellular networks, 5G EMF measurements, coverage analysis.

I. INTRODUCTION

THE DEPLOYMENT of 5G networks is currently an on-going step in many countries in the world - including Italy as well. Although the benefits of 5G are well understood and recognized - mainly in terms of capacity and latency improvements -, the installation of base stations supporting 5G functionalities is still a subject of debate [1], [2]. Not surprisingly, the "5G exposure" term triggers sentiments of anxiety in part of the population [2], mainly because the ElectroMagnetic Field (EMF) from 5G next-generation Node-Bs (gNBs) is believed to be higher compared to the one radiated by pre-5G technologies (e.g., 2G/3G/4G) [3].

In this context, measuring the exposure from 5G gNBs under operation is a fundamental task to control the deployment of 5G and its influence on the EMF levels. On one side, in fact, we can better understand the impact of this technology under practical/realistic conditions (see, e.g., [4]), especially when new frequencies - not necessarily used by pre-5G technologies - are adopted (e.g., below 6 [GHz] and/or mm-Waves). On the other side, we can investigate whether 5G substantially increases the exposure w.r.t. legacy cellular generations - an allegation frequently circulating among the opponents to 5G.

Although the measurement of EMF levels has a crucial importance during (and after) the installation of a new base

station, performing extensive campaigns from commercial 5G gNBs is a challenging task, due to a variety of reasons. First, 5G exploits new features (e.g., extensive beamforming techniques with spatial/temporal beam management [5]), which were used by previous generations up to a limited extent. Second, new portions of the spectrum are dedicated to the 5G signal and, in some cases, new spectrum allocation techniques (e.g., Dynamic Spectrum Sharing (DSS) [6]) are adopted to share the 4G bandwidth for both 4G and 5G signals. Third, the exploitation of high frequencies (even below 6 [GHz]) suggests that propagation effects (due, e.g., to different sight conditions and/or different distances from the serving gNB) have a large impact on the exposure levels [7]. Consequently, the exposure generated by 5G gNBs strongly depends on the specific location where EMF is evaluated.

Ideally, the best solution to evaluate exposure from a commercial 5G gNB would be to perform a measurement campaign with a Spectrum Analyzer (SA) over a massive number of locations in the serving area of the cell. As reported by different measurement standardization bodies (see, e.g., [8] for the Italian case), the exploitation of an SA allows performing NarrowBand (NB) 5G measurements (to differentiate the contribution of 5G w.r.t. legacy generations), as well as clearly identifying the contributions of all the EMF sources that are sensed in the measurement location. Although portable SAs are already available on the market (see, e.g., [9]), their massive usage over the territory is a challenge. In particular, such devices are constrained by a rather limited battery duration - often coupled with long recharging times - which tend to limit the number of measurements that can be performed with a single device. In addition, the cost of a single professional portable SA is still pretty high, due to different options that are required for a thorough assessment of 5G exposure, which range, e.g., from the need of performing real-time analysis over large spectrum portions, as well as demodulation of the 5G signal to collect 5G network parameters (e.g., cell ID, beam index, power received for each beam, etc.). In this context, acquiring multiple SAs to spatially parallelize the measurements is rather unaffordable from a monetary cost point of view.

The goal of this paper is therefore to face the aforementioned issues and answer the following question: Is it possible to massively sense the exposure from a commercial 5G deployment *while* limiting the locations where the SA-based measurements are performed? To answer this question, we adopt a novel approach that integrates multiple equipment tools: one portable SA, one portable Wide Band (WB) EMF meter and one 5G User Equipment (UE) (a.k.a. 5G smartphone). Rather than massively performing the measurements with the SA over the whole territory under consideration, we perform this task with the 5G UE. In particular, we collect geo-referenced values of the received power on the control channel from the 5G network (by measuring the Synchronization Signals - Reference Signal Received Power (SS-RSRP) metric). In the following step, we select the locations to perform detailed measurements with the SA and the EMF meter. This selection is based on the information derived from the deployment under consideration (including the orography of the territory) *and* the analysis of the SS-RSRP metric massively collected with the 5G UE during the previous step.

Results, measured from a commercial 5G deployment installed in an Italian town, point out several interesting aspects. First of all, 5G exposure is at most equal to 0.7 [V/m] in the scenario under consideration - which included traffic generated by other users. Moreover, 5G generally represents a small fraction of the total EMF exposure in most of the measurement locations. Second, we observe a strong correlation between the propagation conditions (e.g., in terms of Line-of-Sight (LOS) vs. Non-Line of Sight (NLOS), distance from the serving sector, difference in altitude w.r.t. 5G installation) and the measured 5G EMF level. Third, the exploitation of the integrated approach allows easily detecting exposure outliers and unexpected exposure behaviors, including, e.g., locations covered by 5G through the DSS functionality over 4G frequencies as well as zones simultaneously covered by multiple 5G sectors. Fourth, the 5G SS-RSRP metric measured with the 5G UE is a very good proxy of the Real Time (RT) channel power measured by SA over the 5G spectrum of a given cell and a given operator. Fifth, the total estimated power that is radiated by each 5G sector is lower than 130 [W] per sector, even by assuming no reflection effects and low antenna numeric gains.

The rest of the paper is organized as follows. Section II overviews the related works. Section III presents our measurement methodology. Section IV reports the results obtained from the analysis of the performed measurements. Section V concludes the work and presents possible future research activities. Finally, for the sake of clarity, the acronyms introduced throughout the paper are also expanded in Appendix A.

II. RELATED WORKS

The measurement of exposure from cellular networks is a central point covered by International Telecommunication Union (ITU) recommandations [10], [11], International Electrotechnical Commission (IEC) standards documents [12], [13], national standardization bodies [8] and national exposure regulations [14]. Despite we recognize the importance of such previous resources, we point out that our work is focused on a different aspect, i.e., the massive evaluation of exposure over the territory by limiting the number of locations where the SA has to be used. However, we integrate in our methodology measurement settings/procedures that are included in relevant standards (e.g., [8]). Moreover, we stress the fact that our goal is not to compare the measured exposure levels against the maximum EMF limits defined by law - a step that would require to significantly increase the amount of time

spent for the measurement of the electric field in each location.[1]

The adoption of the SA for the assessment of exposure from 5G cellular networks is advocated by [15]–[19]. To this aim, Aerts *et al.* [15] propose an SA-based measurement methodology to evaluate the time-averaged instantaneous exposure and the theoretical maximum one. More in depth, all the measurement locations are in LOS w.r.t. the serving gNB, and in general in proximity to the base station. In contrast to [15], in this work we propose an approach based on the exploitation of multiple equipment (portable SA, portable EMF meter and 5G UE) to limit the number of locations where SA tests are performed. In addition, the authors of [15] evaluate 5G exposure also in the presence of data traffic generated on purpose by one 5G UE. This step was surely meaningful in [15], as the 5G infrastructure was not massively used by other 5G terminals at that time. Differently from [15], in our work we evaluate the exposure of a commercial 5G deployment "as is", since 5G is becoming a service widely used by users at the time of preparing this manuscript. This hypothesis is practically confirmed in the scenario that we consider, i.e., the 5G spectrum measured in different locations reveals a non negligible amount of 5G traffic generated by users. Eventually, Aerts *et al.* expand [15] in [16], by moving their analysis to a commercial 5G deployment in Switzerland. Interestingly, the authors demonstrate that the exposure from the 5G network is rather limited - a conclusion that is also shared by our work. In contrast to [16], we shed light on the exposure over the whole extent of the gNB coverage area (i.e., not only in locations in LOS), which may be meaningful for other purposes (e.g., UE uplink power assessment, coverage analysis) apart from gNB exposure evaluation. In addition, we shed light on the outliers and unexpected deviations that emerge, due, e.g., 5G coverage provided by DSS over 4G frequencies as well as overlapping 5G sectors - a step that has not been investigated by [15], [16]. Moreover, another novelty of our work is the cross-validation of the measurements sensed by different instruments (e.g., 5G UE and SA), as well as the analysis of the 5G parameters that have been decoded through the SA.

Eventually, [17]–[19] propose and evaluate SA-based measurement techniques to measure the instantaneous EMF radiated by 5G gNB *and* to extrapolate the maximum one. Clearly, our work is rather orthogonal w.r.t. [17]–[19], since we focus on the massive evaluation of exposure over the whole extent of the gNB coverage area, by adopting an integrated approach that allows limiting the number of locations in which SA-based tests are performed. Obviously, the methodology of [17], [18] could be applied in the measurement locations selected by our work to compute the maximum achievable exposure.

1. In Italy, for example, the comparison of the average field strength against the limits has to be done by averaging the measured EMF levels over a long time-scale, i.e., typically 24h for residential areas.

Other alternative approaches to evaluate the exposure from a 5G cellular network are investigated by [20]–[22]. More in depth, Colombi *et al.* [20] adopt a network-assisted technique in which the transmission power of a set of commercial gNBs is continuously monitored. In contrast to them, our approach does not require any interaction with the operator. Moreover, we target the exposure evaluation over the territory - although we also estimate the power transmitted by the 5G gNB. Another technique to evaluate 5G exposure is proposed by Lee *et al.* in [21]: in this case, the authors monitor the power transmitted by the 5G UE and the SS-RSRP from the serving gNB. Differently from [21], we target a multi-equipment approach based on measurement performed with SA, EMF meter and 5G UE to evaluate the exposure from cellular base stations. Moreover, we explicitly investigate the impact of the measurement location (e.g., in terms of distance from the serving gNB and sight conditions) on the obtained results - a step that was not considered by [21]. Eventually, Carciofi *et al.* [22] point out the need of performing dynamic measurements with EMF meters to massively collect information about the exposure over the territory. Differently from [22], in this work we adopt a 5G UE (and not the EMF meter) to perform this task. In particular, we show that the SS-RSRP metric collected with the smartphone is a good proxy of the exposure radiated by a 5G gNB. Nevertheless, in line with [22], we employ the EMF meter to evaluate the total exposure in each measurement location.

Finally, other measurement tools (different from the ones used in this work) can be exploited to measure 5G coverage- and exposure-related metrics. More in depth, dedicated 5G network scanners [23] are able to collect 5G decoded parameters, which may be useful for a thorough (and detailed) exposure characterization. We leave the integration of such devices in our framework as a future work, e.g., in combination with the SS-RSRP measurements recorded with the 5G UE over the territory.

III. MEASUREMENT METHODOLOGY

We divide the presentation of our measurement technique in the following steps: *i*) motivations and consequently measurement goals that have to be addressed, *ii*) feature comparison among the available equipment, and *iii*) presentation of the integrated approach for the massive measurement of 5G exposure. In the following steps, we shed light on each of the aforementioned points.

A. MOTIVATIONS AND GOALS

Our primary motivation (and goal) is the evaluation of the 5G exposure over the territory from a commercial 5G deployment, by limiting the number of locations where the SA is employed. However, other interesting aspects that further stimulate our work include the following questions: *i*) Which is the exposure of 5G in comparison to other wireless technologies? *ii*) How does exposure is affected by the specific measurement location? *iii*) If the smartphone does not show

5G connectivity, can we conclude that there is absence of 5G exposure? and *iv*) If the smartphone shows 5G connectivity, does it really mean exposure over dedicated (and new) 5G frequencies?

To tackle the aforementioned aspects, we derive a set of measurement goals. First of all, the measurement has to be *selective*, meaning that we need to separate the exposure contributions from the different technologies, with a special focus of 5G. Second, the measurement has to be *comprehensive*, meaning that, apart from the single contributions, we should be able to measure the total exposure in the location. Third, the measurement has to be *reliable*, meaning that we should be able to limit the presence of errors that may invalidate the results. Fourth, the measurement has to be *explainable*, meaning that similar metrics measured with different tools have to be in accordance to each other, or - in case of deviations - valid explanations for the observed differences have to be provided.

B. EQUIPMENT COMPARISON

Table 1 reports a comparison of the available measurement equipment in terms of model, installed software/hardware options, available measurement metrics that are relevant in the context of 5G, main equipment advantages as well as challenges.

Focusing on the SA, the HardWare (HW) is capable of spectrum analysis up to 32 [GHz], while the installed options include Real Time Spectrum Analysis (RTSA) up to 100 [MHz] of bandwidth, measurement of 5G NR decoded metrics, gated sweep and Global Positioning System (GPS) receiver. Such features are able to satisfy the requirements for measuring 5G signal currently available in Italy, which is generated by gNBs operating over 3.6-3.78 [GHz] frequencies and a maximum BandWidth (BW) equal to 100 [MHz] per operator.[2] The set of metrics that can be measured/extracted by employing the SA is huge, ranging from the temporal evolution of the spectrum over time (i.e., the spectrogram) both in RT over a maximum BW equal to 100 [MHz] or not in real time over wider BW, to the total power received over the 5G channel (either in RT from overlapping 5G spectra from multiple gNBs/sectors or from a 5G decoded spectrum of a single gNB/sector), to decoded 5G NR network parameters that include cell ID, beam index and SS-RSRP.

The SA is then connected to a single-polarized (directive) antenna. The reason why a single polarized directive antenna is a good choice in the measurement campaign reported in the article (finalized to verify the radio coverage as well as EMF qualitative values) is related to the use of massive Multiple-Input Multiple-Output (MIMO) antennas in 5G technology. In particular, Synchronization Signal Block (SSB) burst transmission is based on the use of multiple radiation beams - each of them rather narrow - and typically associated to a single SSB of the burst set. A directive antenna allows easily identifying the most powerful SSB in the receiver point with great precision and its use is preferable w.r.t. omnidirectional antennas that are typically characterized by lower gain values. However, there are some issues that are introduced when a directive antenna is employed. In particular, the contributions from the SSB from directions which are not in direct LOS with the gNB might be neglected. In addition, the radiation pattern from the SSB might be different for different polarizations (unless the antenna is rotated some contributions from the gNB are not measured).

In our evaluations, we employ a directive antenna that is oriented towards the position of the serving gNB sector, in order to maximize the amount of captured exposure. Clearly, when the scope of the measurement is the verification of exposure against the maximum limits, a different antenna has to be used (i.e., typically working on three axis and on dual polarization) - but this is not the situation targeted in our work.

Obviously, a major advantage in adopting the SA is the measurement flexibility: with this tool, in fact, both NB (i.e., selective) and WB measurements can be performed. In addition, the contributions from multiple technologies (5G vs. not 5G sources) and/or multiple operators radiating in the same area can be easily characterized. Moreover, the tuning of the SA parameters allows reaching the highest level of detail in the exposure assessment. Clearly, the main drawback of the portable SA is the duration of the battery, which tends to rapidly reach low values, especially when multiple metrics (e.g., spectrogram, RT spectrum, 5G NR parameters) are sequentially evaluated in the same location.[3] Moreover, the equipment maneuverability is rather limited, since the SA weight equals 5.4 [kg] (a not negligible value) and the external receiving antenna has to be hand-held or put on a tripod.

The second equipment reported in Table 1 is the portable EMF meter. Compared to the SA, the set of metrics sensed by this tool is rather limited, being the average EMF level (in terms of V/m) the main information that can be retrieved. Clearly, a WB EMF meter can not distinguish among the different EMF sources radiated over the same location.[4] However, the total electric field strength is a useful information for our analysis, as, in this way, we can compare the selective measurements retrieved by the SA against the total exposure measured by the EMF meter (but

2. 5G gNBs operating on frequencies close to mm-Waves are not commercially available in Italy at the time of preparing this article. However, the measurement over such very high frequencies is still possible with the available SA, i.e., by replacing the receiving antenna with another one covering also the frequencies close to mm-Waves (26.5-27.5 [GHz] in Italy).

3. In our tests, we experience a battery duration even shorter than two hours.

4. In this work, we use the WPF8 probe [26], which senses the total EMF over the range 100 [kHz]-8 [GHz]. The manufacturer also provides the WPT probe [27], which measures total EMF over 2G/3G/4G frequencies. However, this solution provides only the total EMF over the sensed frequencies (i.e., without distinguishing the contribution of each frequency) and - at the time of preparing this article - it does not include 5G frequencies yet.

TABLE 1. Comparison among the available equipment.

	Model	Installed Options	Relevant Metrics	Advantages	Challenges
Portable SA	Anritsu MS2090A [9] with Aaronia 6080 HyperLog Antenna [24]	SA up to 32 [GHz] 100 [MHz] BW analysis RTSA 5G-NR DL measurements Gated sweep GPS Receiver	Spectrogram RT spectrogram 5G RT channel power 5G NR channel power 5G NR cell ID 5G NR SS-RSRP 5G NR Beam Index	NB and/or WB measurements Measurements from multiple operators/technologies Highest level of detail	Limited battery duration (max 2 hours) Limited instrument maneuverability
EMF Meter	WaveControl SMP2 with probe WPF8 [25]	GPS Receiver	Total EMF Strength	Evaluation of total exposure Long battery duration (hours)	No NB measurements Limited instrument maneuverability
5G UE	Samsung S20+ 5G	Android 11 (1st May 2021) with CellMapper 5.5.1	SS-RSRP (serving cell)	Long battery duration (hours) Highest instrument maneuverability Ease of measurement	Meas. from a single cell No info about total 5G exposure No info about 5G cell ID

however keeping in mind that the antenna of the former is a directive one, while the latter measures the EMF with an isotropic Root Mean Square (RMS) diode technology). In addition, the battery duration of such device is very long (i.e., in the order of hours). However, similarly to the SA, the equipment maneuverability is not very high, as the EMF meter and probe have to be installed on a tripod to perform reliable measurements.

Finally, the last equipment under consideration in Table 1 is a Samsung S20+ 5G UE. Despite the manufacturer advertised the 5G feature starting from the smartphone launch in 2020, 5G connectivity has been made available in Italy only one year later, by upgrading the Android operating system to version 11 (with update release on 1st May 2021). In addition, we install CellMapper v.5.5.1 App to collect geo-referenced SS-RSRP values. Moreover, we select the following options on the CellMapper App: *i*) exportation of the measured data on an external file (in order to perform post-processing analysis), *ii*) recording limited to the 5G parameters (i.e., we skip the recording of pre-5G metrics) and *iii*) minimum recording interval of 1 [s] (i.e., the lowest one). With these settings, we are able to capture the SS-RSRP from the serving cell (and not from other ones possibly covering the same location). Moreover, we do not have (in principle) any indication about the total exposure over the entire 5G spectrum (even by the same operator). Apart from the SS-RSRP, other metrics that are in theory recorded by CellMapper include the mobile operator codes and the cell ID. Focusing on the latter, we have noticed that the cell ID was not recorded/displayed by the App at the time of preparing this paper. We argue that this bug may be fixed in future releases (as we verified that the cell ID of pre-5G technologies was correctly sensed by CellMapper), but we had to deal with this issue in our work. Intuitively, in fact, the cell ID is an essential information, which allows associating the recorded value of SS-RSRP to a given gNB (and a given sector of the base station).

C. INTEGRATED APPROACH FOR MASSIVE MEASUREMENTS

Having understood that a single device is not suitable for the massive evaluation of 5G exposure, we have developed an integrated approach based on the measurements serialization,

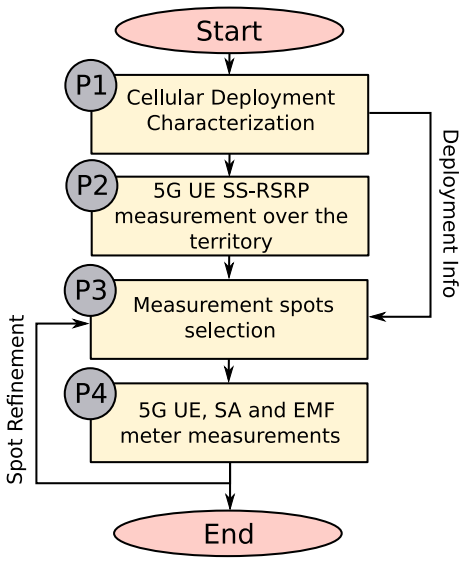

FIGURE 1. Main steps of the proposed integrated approach for massive 5G measurements.

by jointly exploiting the portable SA, the WB EMF meter and the 5G smartphone. Intuitively, our idea is take advantage of the benefits of each tool, while at the same time addressing their shortcomings, by: *i*) splitting the massive measurement (complex) task over a set sequential phases, subject to different measurement granularity levels, and *ii*) assigning each tool to the most suitable phases(s), by carefully considering the shortcomings of the device.

More formally, Fig. 1 reports the high-level pseudocode of our integrated procedure. The massive measurement is split in the following phases: *i*) cellular deployment characterization, *ii*) measurement of the SS-RSRP metric with the 5G UE over the territory, *iii*) selection of the measurement spots, and *iv*) measurement of detailed exposure parameters by jointly using the SA, the EMF meter and the 5G UE in each measurement location. In the following, we shed light on each of the previous steps.

1) CELLULAR DEPLOYMENT CHARACTERIZATION

During this step, we characterize the network deployment under consideration. In particular, we localize all the cellular installations in an area under consideration by: *i*) querying the Web interface of CellMapper to get the estimated

positions of the base stations for all the Italian operators and all pre-5G technologies, *ii*) driving over the selected area to double check the localization of the estimated installations and/or the presence of other installations (not reported by CellMapper), *iii*) standing at a short distance (around 50-100 [m]) from each installation found in point *ii*) (in LOS conditions), and check with the SA (with RTSA option enabled) the presence of the 5G signal over all the spectrum portions assigned to operators in the 3.6 [GHz]-3.78 [GHz] band used in Italy, *iv*) marking with "5G" ("Other") an installation in which the 5G RT spectrum occupation is consistently higher than (equal to) the noise level. Clearly, the "Other" label is used to mark installations that exploit only pre-5G technologies, while "5G" denotes base stations hosting 5G panels (and eventually also pre-5G equipment). Moreover, in parallel to this step, we also characterize the territory altitude of the selected area by retrieving the Digital Elevation Information (DEI) from [28], as a matrix of pixels storing altitude information. This step is in fact essential to understand the propagation of the 5G signal obseved over the territory, which is (obviously) highly impacted by the orography, e.g., in terms of hills and canyons. The output of P1 is then a set of base station coordinates (either marked with "5G" or "Other") and the DEI for the territory under consideration.

2) 5G UE SS-RSRP MEASUREMENT OVER THE TERRITORY

The second part of our approach consists in massively measuring the SS-RSRP over the territory. As already shown by previous works tailored to 4G network (see, e.g., [29]), a complete Reference Signal Received Power (RSRP) characterization requires a diffuse measurement campaign, due to the different propagation conditions experienced over the territory, which are in turns reflected in strong changes of the measured RSRP levels. In this work, we proceed as follows: *i*) we start from the installations labeled with "5G" in P1, *ii*) we measure the received SS-RSRP by walking in each and every public street around the 5G installations, *iii*) we cover all the streets around each 5G installation, up to a distance of 800 [m] from the considered gNB.[5] Moreover, we adopt the following settings: *i*) the 5G UE is held by hand at a height of 1.5 [m] from ground level, *ii*) the screen of the smartphone is always powered on, with the CellMapper application opened on top, *ii*) the measurements are taken during late morning/early afternoon hours of working days (i.e., far from off-peak hours). In this way, CellMapper continuously monitors the 5G connectivity, and eventually stores the observed values of SS-RSRP that are geo-referenced over the territory. Despite the always on screen setting may potentially consume an high amount of power, we actually experience battery durations always compatible with the time required to perform each campaign (i.e., 3-4 hours).

5. We manually verify that the distance of 800 [m] is an upper bound to the maximum 5G coverage in our scenario.

At the end of this part, we obtain a sequence of geo-referenced SS-RSRP values. However, the density of such measurements may be not uniform, as, e.g., it happens very frequently to walk over the same street for several times (in order to reach other streets). Therefore, in order to harmonize the measurements, we proceed as follows: *i*) we divide the territory into a set of contiguous squared pixels of size 10×10 [m^2],[6] *ii*) we associate each measurement to the corresponding pixel in *ii*), *iii*) we compute the average SS-RSRP sensed in each pixel (for those pixels having at least two samples) - computed by averaging the RSRP values in [mW], and then reported back to [dBm].

3) SELECTION OF THE MEASUREMENT SPOTS

The following step of our approach is the selection of the spots where we perform more detailed measurements with all the equipment tools used in parallel in each location. As reported in Fig. 1, this step takes as input the characterization of the network deployment (P1), the analysis of the SS-RSRP collected over the territory (P2) and the feedback from already performed measurements over the spots (P4). Therefore, rather than a single sequential step, the selection of the spots is an iterative process over time. In our work, we adopt the following principles to select the measurement points: *i*) locations in close proximity (i.e., up to 250 [m]) from the gNB, *ii*) locations at an intermediate distance from the gNB (i.e., from 250 [m] up to around 500 [m]), experiencing different sight conditions (LOS, NLOS) from P1 and a variegate set of SS-RSRP levels from P2, *iii*) locations in which the measured SS-RSRP level exhibits a strong spike w.r.t. other RSRP measurements taken in the surrounding pixels, *iv*) locations at a distance higher than 500 [m] to verify the presence of the 5G signal and *v*) locations that are supposed to be at the border of a given sector (based on the analysis of the already performed measurements over the territory).

Regarding the cardinality of the measurement spots, such number is (obviously) influenced by the considered network deployment and the type of pursued analysis (e.g., only exposure over locations in proximity to the gNB and/or complete coverage analysis over the territory). In our work, we have found that dozens of measurements spots are required for each gNB, in order to get detailed coverage and exposure information.

4) 5G UE, SA AND EMF METER MEASUREMENTS

The following step is then the measurement of 5G exposure in the selected locations. As reported by Table 2, we split P4 into a sequence of T1-T4 tasks. T1-T3 are sequentially run with the SA, while T4 and T5 are run in parallel to

6. This value is inline with the minimum size of the roads in the considered scenario. Values higher than 10 [m] per side may result into RSRP values from neighboring roads - possibly subject to different propagation conditions - (wrongly) assigned to the same pixel. In a similar way, values lower than 10 [m] may result in a number of measurements per pixel not very high (thus limiting the benefits of the SS-RSRP averaging).

TABLE 2. Evaluation steps performed in P4.

Task	Scope	Tool	Goal	Settings	Equipment Output	Post-processing Metrics
1	Spectrogram Analysis	Portable SA	Coarse Evaluation of EMF Sources	Range: 680 [MHz]-4 [GHz] Detector Type: Peak Meas. Type: Max Hold Sweep samples: 4000 Duration: 1 [min]	NB PD vs. time	Total 5G PD Total 2G/3G/4G PD Tot. PD from other sources
2	5G Channel Analysis	Portable SA	Evaluation of 5G Exposure	Range: 3600 [MHz]-3620 [MHz] Detector Type: Peak Meas. Type: Clear/Write Sweep samples: 501 RTSA option selected Duration: 1 [min]	NB received power vs. time	5G RT channel power 5G RT PD Avg. RT EMF Strength
3	5G NR Analysis	Portable SA	Evaluation of 5G parameters	Center frequency:3.61 [GHz] Channel BW: 20 [Mhz] SCS: 30 [kHz] SSB Offset:-5.2 [MHz] Detector Type: Peak Meas. Type: Average Number of avg. samples: 1000 Sweep samples: 501	5G NR channel power 5G SS-RSRP 5G cell ID 5G beam index	5G SS-RSRP (strongest beam) Beam index (strongest beam)
4	Total EMF Analysis	EMF Meter	Evaluation of Total Exposure	Sampling Rate: 0.5 [s] Duration: 1 [min]	Avg. EMF strength	-
5	Smartphone Analysis	5G UE	Qualitative Eval. of 5G Exposure	Record only 5G SS-RSRP Min. rec. interval: 1 [s]	SS-RSRP (serving cell)	Geo-referenced SS-RSRP pixelization

T1-T3 with the EMF meter and the 5G UE, respectively. In the next paragraphs, we formally present each task.

Task 1 (Spectrogram Analysis): The goal of T1 is to perform a coarse (and rapid) measurement to identify the different EMF sources radiating over the locations. In line with the SA-based approach of [15], we set a large span, covering the frequencies between $f^{\text{T1}}_{\text{MIN}} = 680$ [MHz] and $f^{\text{T1}}_{\text{MAX}} = 4$ [GHz].[7] The value of $f^{\text{T1}}_{\text{MIN}}$ corresponds to the minimum frequency measured by the receiving antenna, while $f^{\text{T1}}_{\text{MAX}}$ is set to include all the 5G frequencies of currently installed gNBs in Italy (including an additional margin of 220 [MHz] to the highest 5G frequency). We then impose a number of sweep samples N_{SAM} equal to 4000, which is the maximum available value by the SA. In this way, we minimize the frequency spacing Δ_f between two consecutive sweep points, resulting in $\Delta_f = 8.3 \cdot 10^5$ [Hz]. We then allow the SA automatically setting both Resolution BandWidth (RBW) and Video BandWidth (VBW), resulting in RBW = 10 [MHz] and VBW = 3.33 [MHz], respectively. With these setting, the observed sweep time is equal to 260-300 [ms]. Eventually, we adopt a "Peak" type detector and a "Max Hold" measurement type [15]. In this way, the peak of received power for each frequency sample is stored (during the measurement window), and the maximum value over time for each frequency is saved.

The output of the SA is a matrix of time-referenced frequency-selective power density values $\rho_{(f,t)}$ over the range $f \in [f_{\text{MIN}}, f_{\text{MIN}}]$ and $t \in [t_{\text{START}}, t_{\text{END}}]$.[8] Given the $\rho_{(f,t)}$ values, we then apply a set of post-processing scripts (developed in Bash and AWK script languages) to retrieve the following information: *i*) total Power Density (PD) observed over 5G frequencies, *ii*) total PD observed over 2G/3G/4G frequencies, *ii*) total PD observed over EMF sources whose operating frequencies are not included in *i*)-*ii*).

Focusing on *i*), we proceed as follows. First, we select the last temporal column t_{END} from $\rho_{(f,t)}$ (corresponding to the max-hold over the entire measurement period). Second, we consider only the frequency samples falling in the interval $\mathcal{F}_{5\text{G}} = [f_{5\text{G-MIN}}, f_{5\text{G-MAX}}]$, where $f_{5\text{G-MIN}} = 3.6$ [GHz] and $f_{5\text{G-MAX}} = 3.78$ [GHz] (i.e., the band currently adopted in Italy for 5G). Third, we compute the total PD over 5G frequencies as:

$$\Lambda_{5\text{G}} = \frac{1}{\kappa \cdot \text{RBW}} \sum_{f \in \mathcal{F}_{5\text{G}}} \rho_{(f,t_{\text{END}})} \cdot \Delta_f \qquad (1)$$

where $\kappa = 1.2$ is the ratio between Equivalent Noise Bandwidth (NBW) and the RBW during T1 (i.e., a conservative setting w.r.t. the ones reported by [30]), while $\Delta_f =$ [Hz] is the already introduced frequency spacing.[9] We refer the interested to reader to Appendix B for a detailed explanation on how we retrieved Eq. (1).

Focusing on *ii*)-*iii*), we compute the total PD over 2G/3G/4G (denoted as $\Lambda_{\text{2G-3G-4G}}$) and the total PD over other sources (denoted as Λ_{OTHER}) exactly as in Eq. (1), by simply replacing $\mathcal{F}_{5\text{G}}$ with $\mathcal{F}_{\text{2G-3G-4G}}$ (the set of frequencies used by 2G/3G/4G) and with $\mathcal{F}_{\text{OTHER}}$ all the other frequencies not assigned to 2G/3G/4G/5G, respectively.

Task 2 (5G Channel Analysis): The goal of T2 is to precisely characterize the exposure experienced over the

7. An alternative approach adopted by national protection agencies to precisely dissect the exposure contributions consists in adopting small spans, with central frequencies corresponding to the one used by each operator in each technology (2G/3G/4G). We refer the interested reader to [8] for an overview of such measurement techniques (including the Video BandWidth (VBW) and Resolution BandWidth (RBW) settings). Although such approach allows retrieving very detailed (and reliable) measurements about all exposure contributors, it also consistently increase the time required to perform the measurement in each location - a sensitive metric that we target to reduce in our analysis, in order to preserve the SA battery duration.

8. We preliminary upload on the SA the numerical values of antenna factor that are available on the antenna manufacturer website. In this way, the SA is able to return the measured power density $\rho_{(f,t)}$ for each frequency.

9. All the terms appearing in Eq. 1 are expressed in linear and with plain units ([W/m^2] for PD, [Hz] for frequencies)

entire 5G channel. To this aim, we consider a small span (at maximum equal to 80 [MHz]) and we activate the RT option of the SA. The parameters reported in Table 2 for T2 refer to a single 5G operator exploiting 20 [MHz] of BW (i.e., the Italian WindTre operator) - which is the one that provided 5G coverage in the scenario that we consider.[10] In addition, we set the type detector to "Peak"[11] and the measurement type to "Clear/Write", respectively. With these settings, the SA records the peak over the RBW window for each sweep. However, the maximum is only computed during each sweep, i.e., no state information is transferred between one sweep and the following one. Moreover, the number of samples per sweep is set to the maximum value ($N_{\text{SAM}} = 501$), while the RBW and VBW are automatically set to 181.818 [kHz] and 60.606 [MHz], respectively. With these settings, the observed sweep time is equal 50-60 [ms]. Eventually, we perform the measurement over a short temporal interval of one minute.

The output produced by the SA at the end of the measurement is a matrix of received power values $\sigma_{(f,t)}$, where $f \in [3.6, 3.62]$ [GHz] and $t \in [0, 60]$ [s]. Given the frequency-selective received power, we compute the 5G RT channel power $C_{\text{5G-RT}}$ by: *i*) averaging each frequency sample over all the sweeps, and *ii*) applying the normalization procedure of [8] to compute the channel power. More formally, $C_{\text{5G-RT}}$ is expressed as:

$$C_{\text{5G-RT}} = \frac{B_{\text{5G}}}{\kappa \cdot \text{RBW}} \frac{1}{N_{\text{SWP}} \cdot N_{\text{SAM}}} \sum_{f \in \mathcal{F}_{5G}} \sum_{t \in \mathcal{T}} \sigma_{(f,t)} \quad \text{[W]} \quad (2)$$

where $B_{\text{5G}} = 20$ [Mhz] is the considered 5G BW, $\kappa = 1.2$ (as in T1), $\text{RBW} = 18.181 \cdot 10^5$ [Hz], $N_{\text{SWP}} = 501$ and N_{SAM} is the number of samples (around 1160) saved by the equipment during the one minute measurement window.

The following metric that we extracted is the total 5G RT PD, denoted as $\Lambda_{\text{5G-RT}}$. In particular, the PD over each sample in (f, t) is first extracted by simply dividing $\sigma_{(f,t)}$ for the effective area of the antenna A_f, and then we apply the same averaging/normalization factors already reported in Eq. (2). More formally, $\Lambda_{\text{5G-RT}}$ is expressed as:

$$\Lambda_{\text{5G-RT}} = \frac{B_{\text{5G}}}{\kappa \cdot \text{RBW}} \frac{1}{N_{\text{SWP}} \cdot N_{\text{SAM}}} \sum_{f \in \mathcal{F}_{5G}} \sum_{t \in \mathcal{T}} \frac{\sigma_{(f,t)}}{A_f} \left[\text{W/m}^2\right] \quad (3)$$

with the same parameters setting as in Eq. (2). Clearly, the effective area A_f is expressed as:

$$A_f = \frac{\lambda_f^2 \cdot G_f^{\text{REC}}}{4\pi} \quad \left[\text{m}^2\right] \quad (4)$$

10. In case of multiple operators simultaneously providing 5G coverage over the same territory, the steps reported in T2 have to be repeated for each 5G frequency range assigned to each operator.

11. As reported by [15], the "Root Mean Square (RMS)" detector is the recommended choice to assess the power density contribution within a certain bandwidth. In our measurements, we use a "Peak" detector, as this setting was the default choice of the instrument. We plan to investigate the impact of RMS detector as a future work.

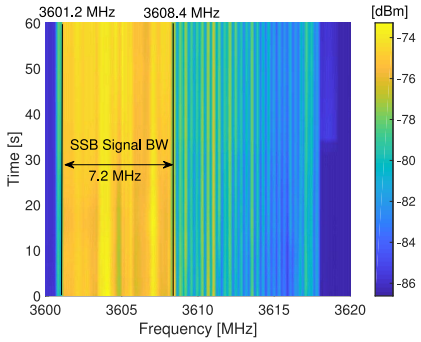

FIGURE 2. Real time spectrogram of the 5G channel recorded in a location in close proximity to the gNB. A bandwidth of 7.2 [MHz] is measured for the SSB signal, spanning from 3601.2 [MHz] up to 3608.4 [MHz]. The SSB offset is therefore set to −5.2 [MHz] w.r.t. the central frequency of 3610 [MHz].

where λ_f [m] is the wavelength of frequency f, while G_f^{REC} is the gain of the receiving antenna over frequency f, which is computed as:

$$G_f^{\text{REC}} = \left(\frac{9.73}{\lambda_f \cdot 10^{\alpha_f/20}} \right)^2 \quad (5)$$

where α_f [dB/m] is the antenna factor of the antenna over frequency f, which has been downloaded from the manufacturer's website [24].

Finally, the third metric that we extracted is the total 5G RT EMF field strength $E_{\text{5G-RT}}$, which has been retrieved by assuming to always operate under far field conditions from the considered gNB. Consequently, $E_{\text{5G-RT}}$ is equal to:

$$E_{\text{5G-RT}} = \sqrt{\Lambda_{\text{5G-RT}} \times \Omega} \quad (6)$$

where $\Omega = 376.730$ [Ohm] is the free-space wave impedance.

Task 3 (5G NR Analysis): During this task, we set the SA to decode the 5G signal and extract different useful metrics that are narrowed on 5G and cell-selective. In more detail, we need to identify the range of frequencies in which the information about the control channel (including the SSB block) is transmitted. Such information is in fact mandatory to set the SSB offset w.r.t. the central frequency of the 5G channel in the SA and therefore allowing the decoding of the 5G signal. Finding the SSB signal BW is not trivial - especially when the channel is also used to transfer traffic data, whose power tends to be higher w.r.t. the one used to transmit the control information [31]. In this work, we extract the SSB signal BW by measuring the values of $\sigma_{(f,t)}$ in RT over the 5G channel at a location in close proximity (less than 200 [m]) w.r.t. the gNB position and in LOS conditions.[12] We have found that, in many locations close to the gNB, the SSB signal BW tends to be rather identifiable, as reported in Fig. 2. In particular, we measured an SSB signal BW equal to 7.2 [MHz], spanning from $f_{\text{SSB-MIN}} = 3601.2$ [MHz] up

12. The equipment also offered an automatic searching for the SSB offset, which however did not provide any outcome (even after waiting for several minutes), at the time of performing the measurements.

to $f_{\text{SSB-MAX}} = 3608.4$ [MHz].[13] Since the central frequency $f_{\text{5G-CTR}}$ is equal to 3610 [MHz], the SSB offset $O_{\text{5G-SSB}}$ is simply computed as:

$$O_{\text{5G-SSB}} = -\left[(f_{\text{5G-CTR}} - f_{\text{SSB-MAX}}) + \frac{f_{\text{SSB-MAX}} - f_{\text{SSB-MIN}}}{2}\right] \tag{7}$$

thus resulting in $O_{\text{5G-SSB}} = -5.2$ [MHz].

Apart from $O_{\text{5G-SSB}}$ and $f_{\text{5G-CTR}}$, the other parameters listed in Table 2 that are needed to decode the 5G signal include the BW (obviously set to 20 [MHz] for the considered operator) and the SubCarrier Spacing (SCS), which is set to 30 [kHz] - a common setting for all the Italian operators operating in sub-6 GHz 5G frequencies.[14] When all these parameters are set on the SA, the equipment start synchronizing and demodulating the 5G signal.

After checking that the SA correctly decodes the 5G signal, we collect the following metrics: *i*) 5G cell ID, *ii*) 5G NR (decoded) channel power, *iii*) 5G SS-RSRP and beam index for each sensed beam. Interestingly, the 5G channel power retrieved in this step is selective over the measured cell ID. In this way, we can distinguish the channel power contribution solely due to the cell displayed by the SA w.r.t. the 5G RT channel power computed in T2 (which may results from the superposition of overlapping cells radiating over the same location). Differently from T2, the channel power in T3 is directly produced as output by the SA, by setting the following measurement input parameters: "Peak" type detector, "Average" over the past 1000 samples and a number of sweep points N_{SWP}. Moreover, we adopt a short measurement window of 15 [s] to compute the average channel power. In this way, we aim at comparing two different methodologies to evaluate the channel power: *i*) a decoded-based technique over a very short time period in T3, against *ii*) an encoded technique in RT over a longer time period in T2.

Focusing on the post-processing steps, we simply compute the best beam index observed in the measurement window of 15 [s] and the corresponding SS-RSRP value, for each measurement location.

Task 4 (Total EMF Analysis): The goal of this task is to measure the average EMF in the measurement location with the WB EMF meter. Fig. 3 reports an example of the measurement in T4, which are taken in parallel to T1-T3. In more detail, the EMF is placed on tripod, on a vertical height of 1.5 [m] above ground, and at distance of around 2 [m] from the SA. The meter is equipped with a WB probe [25], which measures the EMF (in terms of total field strength), over all the frequencies in the range 100 [kHz]-8 [GHz]. We then impose a sampling rate of 0.5 [s] (i.e., the minimum one), a measurement window of 1 [m]. With such settings, the instrument automatically returns the average EMF measured over the window.

13. The value of SSB BW corresponds to a numerology equal to 1, i.e., a 30 [kHz] Sub-Carrier Spacing (SCS). This can be easily verified since the SSB is made of 240 subcarriers and therefore the SSB BW is equal to 240×30 [kHz] $= 7.2$ [MHz].

14. The SCS can be also rigorously derived by dividing the total SSB BW (7.2 [MHz]) by the number of SSB subcarriers (240), yielding to SCS $= 30$ [kHz].

FIGURE 3. Example of parallelization of task T4 (right - EMF meter) and tasks T1-T3 (left - portable SA) in a measurement location.

Task 5 (Smartphone Analysis): The last step that is performed during Phase 4 is the collection of the SS-RSRP values with the 5G UE, by adopting the same settings and the post-processing pixelization already done during Phase 2. In this way, we keep collecting the SS-RSRP values in parallel to T1-T4, in order to increase the number of samples recorded in each measurement location.

IV. RESULTS

In this section, we apply the proposed integrated approach in a town covered by 5G signal. All the measurements were performed during morning hours (10:00 am - 13:30 am) of working days (Monday through Friday) in May 2021, in order to evaluate the EMF during meaningful (and comparable) traffic/exposure conditions. We divide our analysis in the following steps: *i*) characterization of the 5G deployment, *ii*) 5G UE SS-RSRP and measurement locations, *iii*) 5G exposure over the measurement locations, *iv*) joint analysis and outlier discovery, *v*) distance-based analysis, and *vi*) sector-based analysis.

A. 5G DEPLOYMENT CHARACTERIZATION

The first step is the selection of the area in which a 5G signal is supposed to be available. In this work, we consider an area of around 12.4 [km^2] centered in San Cesareo, a town of nearly 16000 inhabitants located at around 20 [km] far from the city of Rome. We select such area because some news about installation of 5G gNBs already appeared

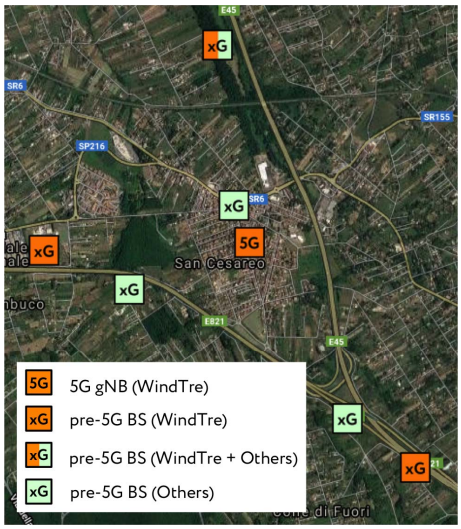

FIGURE 4. Output of Phase 1 - deployment characterization in an area of around 12.4 [km^2], centered over the town of San Cesareo (Italy). The figure reports positioning, supported technologies (including or not 5G equipment), hosted operators (WindTre, Others, WindTre + Others) of each base station over the territory. One base station located in the town center provides 5G services for the WindTre operator.

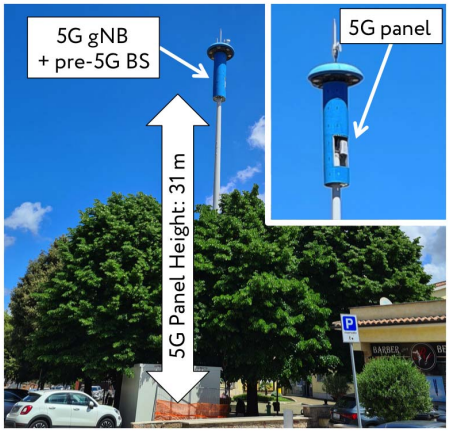

FIGURE 5. 5G gNB under evaluation. The WindTre site includes multiple 5G panels (out of which one uncovered) and different pre-5G equipment (all covered).

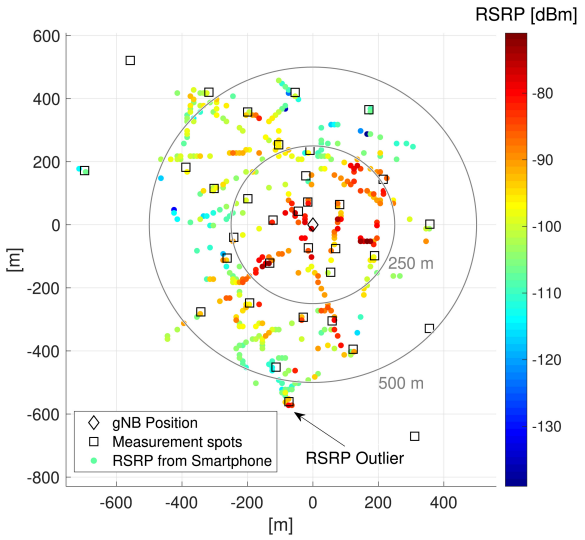

FIGURE 6. Avg. 5G SS-RSRP measured with the smartphone over the territory. The transparent squares denote the measurement locations of the tests in P4 (figure best viewed in colors).

in 2020 on press releases (with several complaints raised by the population). Moreover, no public information about the actual coverage of 5G in the town was available at the time of conducting our analysis (to the best of the authors' knowledge). Therefore, we performed P1 over the territory, whose output is shown in Fig. 4. Interestingly, 5G signal is currently provided by a single gNB installation located in the city center and managed by a single operator (WindTre). We actually found a second installation close to the 5G installation, not supporting 5G functionalities and owned by other operators. Eventually, different pre-5G installations were found outside the area of the city center, all of them not providing 5G signal.

A closer look at the WindTre gNB site is shown in Fig. 5. The base station is placed on an independent pole directly installed at ground in the central square of the town. The 5G panels are placed at a height $H_{\text{gNB}} = 31$ [m] above ground. The gNB is composed by at least one uncovered 5G panel (inset in the figure) and (possibly) other 5G panels that are hidden in the cylindric shell. Intuitively, each 5G panel is supposed to provide coverage over a given sector. The installation includes also other pre-5G equipment, placed at an higher height w.r.t. 5G panels and hidden in the cylinder.[15]

B. 5G UE SS-RSRP AND MEASUREMENT LOCATIONS

After the network characterization step, we have then performed P2 of our approach, i.e., the pervasive measurements of SS-RSRP over the territory with the 5G UE. To this aim, we have used a WindTre Subscriber Identity Module (SIM), with a tariff plan supporting the 5G connectivity. We have then walked through the town of San Cesareo, by covering all the streets up to a maximum distance of around 800 [m] from the gNB (which is supposed to be a meaningful value for the cellular coverage from a single base station in semi-urban areas). Measurements were taken by keeping the smartphone in hand, at an height above ground H_{UE} equal to 1.5 [m]. The total amount of time to complete P2 was around equal to 24 [h] (split over multiple days).

The outcome of this phase is reported in Fig. 6. Several observations can be derived by analyzing the figure. First, the SS-RSRP metric is not constant over the territory, but it is (obviously) subject to large variations, i.e., from around -140 [dBm] up to nearly -70 [dBm]. Second, most of pixels experiencing SS-RSRP > -90 [dBm] are located up to 250 [m] from the gNB location. Third, the SS-RSRP values are not uniformly sensed in the area under investigation. In particular, the overall coverage of the gNB is rather limited, being most of SS-RSRP values observed up

15. These pre-5G technologies were characterized during P4.

to a maximum distance of 500 [m] from the gNB. Fourth, the presence/absence of buildings/obstacles between the 5G UE and the gNB results in abrupt changes of the measured SS-RSRP values, even for pixels pretty close to each other (few dozens meters). Fifth, no SS-RSRP values higher than -80 [dBm] are measured farther than 500 [m] from the gNB, except from an unexpected outlier (highlighted in the bottom part of Fig. 6), which stimulated the placement of a measurement location, in order to perform further analysis.

Fig. 6 also reports the final positioning of measurement locations. In more detail, 34 measurement spots are selected at the end of Fig. 1. Each measurement location required around 10 minutes of time to perform P4 (including the time required to install the equipment, check/tune the measurement scale, perform the tests, and finally uninstall the equipment), thus resulting in approximately 6 [h] to perform the measurements (a task split over multiple days). Intuitively, the majority of measurement points are placed within the area where values of SS-RSRP were sensed with the 5G UE, i.e., at a maximum distance of 500 [m] from the gNB. However, we consider measurement locations also outside the coverage area sensed with the smartphone, in order to verify whether an extremely low 5G signal (lower than the smartphone detection threshold) could be still measured with the SA. Obviously, several evaluation points are placed in locations where high values of SS-RSRP (i.e., > -80 [dBm]) are measured with 5G UE.

Apart from SS-RSRP, we also consider other constraints to select measurement locations. To this aim, we preliminary compute the difference in altitude $\delta_{(p,\text{gNB})}$ between a candidate measurement location placed on a given pixel (at a height of 1.5 [m] above ground) and the 5G panel. $\delta_{(p,\text{gNB})}$ is formally expressed as:

$$\delta_{(p,\text{gNB})} = \left(A_p + H_{\text{UE}}\right) - \left(A_{\text{gNB}} + H_{\text{gNB}}\right) \quad [\text{m}] \qquad (8)$$

where A_p (A_{gNB}) is the pixel (gNB) altitude - retrieved from the DEI in P1, while H_{UE} (H_{gNB}) is the 5G UE (panel) height above ground.

Fig. 7 reports $\delta_{(p,\text{gNB})}$ for all the pixels p in the area close to the gNB. Interestingly, the considered territory is not exactly plain, thus resulting into a non negligible variation of $\delta_{(p,\text{gNB})}$ over the set of pixels. More in depth, the gNB is surrounded by a set of smooth hills, which are subject to $\delta_{(p,\text{gNB})}$ values close to 0 [m] (especially those ones located on the summits). For example, such favorable propagation condition is experienced in the zone on bottom left of the figure, which is reachable from the gNB through a smooth canyon (reported in the central part of the figure).[16] A second canyon is evident on top left of the figure. In addition, different pixels are located on smooth valleys, subject to $\delta_{(p,\text{gNB})} < 0$. In many cases, such valleys experience NLOS conditions w.r.t. the gNB, due to the presence of summits located in the middle.

16. A canyon is defined as a valley surrounded by smooth hills on both its sides.

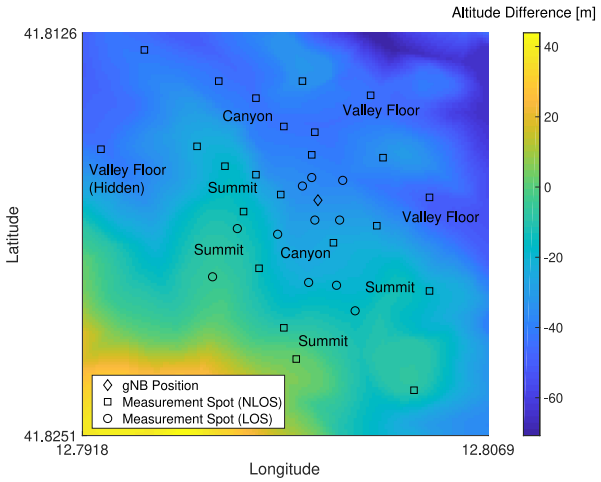

FIGURE 7. Altitude difference between 1.5 [m] above ground level for each pixel and the altitude of the 5G panel. The figure reports also the measurement locations and their sight conditions w.r.t. the gNB (figure best viewed in colors).

FIGURE 8. Measurement location 3 with LOS propagation conditions w.r.t. the 5G gNB.

Since the variation of $\delta_{(p,\text{gNB})}$ is not negligible, we have arranged different measurement locations in order to sample summits, valleys, canyons in our scenario - up to a maximum distance of around 800 [m] from the gNB. The positioning of the measurement locations w.r.t. $\delta_{(p,\text{gNB})}$ is also highlighted in Fig. 7. To this aim, Fig. 8 reports one representative case, in which the measurement location is placed on a summit, in clear LOS w.r.t. the gNB. Other measurement locations sharing similar propagation conditions are reported on bottom left and bottom right of Fig. 7. Obviously, it is expected that such points will be subject to a non-negligible 5G exposure, due to the favorable propagation conditions w.r.t. the gNB.

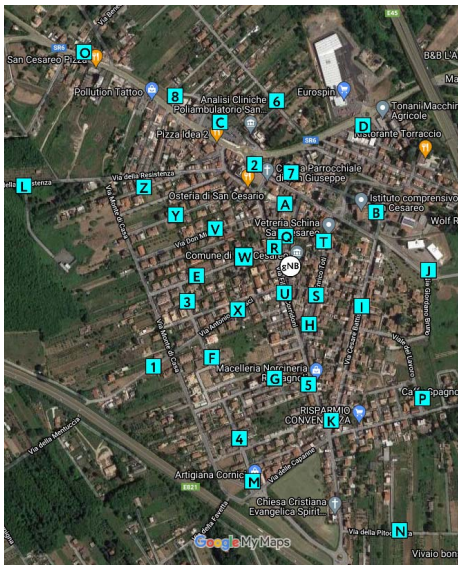

FIGURE 9. Measurement locations over the territory (figure best viewed in colors).

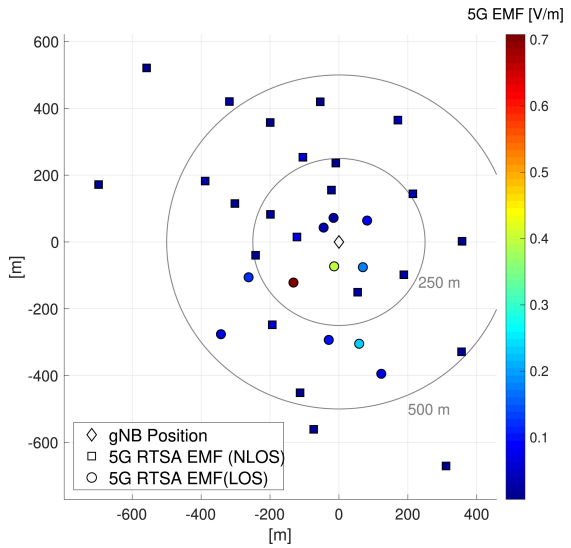

FIGURE 10. 5G EMF measured with the real-time spectrum analyzer over the measurement points (figure best viewed in colors).

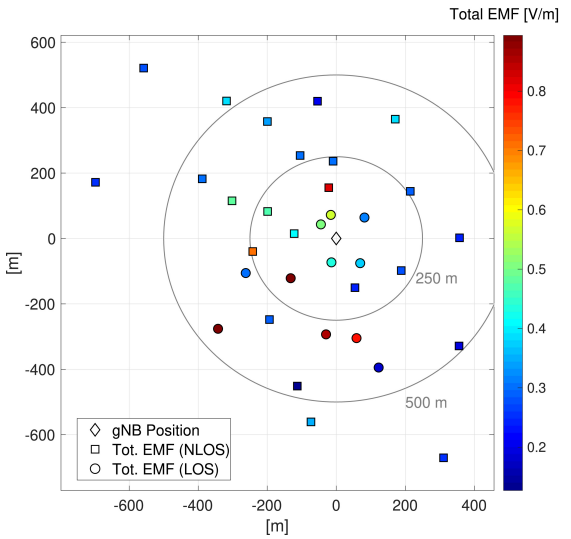

FIGURE 11. Total EMF measured with the wide-band EMF probe over the measurement points (figure best viewed in colors).

Finally, Fig. 9 highlights the measurement locations over a satellite image of the territory. For each location, a unique identifier has been assigned. Two considerations hold by analyzing the figure. First, most of the locations are placed in residential areas, i.e., areas in close proximity to buildings where people live/work. Second, the territory on center left w.r.t. the gNB is composed by different straight roads in LOS w.r.t. the gNB - a feature contributing to the spreading of the 5G signal over the territory.

C. 5G EXPOSURE OVER THE MEASUREMENT LOCATIONS

In the following step, we perform P4 over the measurement locations. In particular, the whole procedure required around 9 hours to be completed, again split over different working days of May 2021. We then address the following question: Which is the exposure generated by the 5G gNB? To this aim, Fig. 10 reports the average 5G RT EMF measured with the SA during T2 of P4. Interestingly, the 5G exposure is typically lower than 0.2 [V/m] for most of locations. By mutually comparing Fig. 10 against Fig. 7 the locations experiencing the highest EMF values are those ones in LOS w.r.t. gNB, either in close proximity to the gNB, or placed on summit conditions like in Fig. 8. However, the 5G EMF exposure appears be rather limited even in those locations, with a maximum EMF equal to 0.71 [V/m].

Given this picture, we target another important question: Is 5G exposure comparable w.r.t. EMF generated by other sources? To answer such question, Fig. 11 reports the total exposure measured with the EMF meter during T4 of P4. Interestingly, the overall EMF generated by all the sources in the territory is rather limited, being the maximum field strength equal to 0.87 [V/m]. However, several differences emerge when comparing the total EMF in Fig. 11 against the 5G one in Fig. 10. In particular, many points on top part of the figure experience a non-negligible total EMF *and* a very low 5G EMF. This difference may be explained by the presence of the second base station in the town (shown in center-to-left part of Fig. 4), which contributes to the exposure of 2G/3G/4G over such locations. Moreover, the zone experiencing the highest exposure is again the one located on bottom center of the figure, which we remind is composed of locations in favorable propagation conditions w.r.t. the central gNB (which also hosts pre-5G equipment).

In order to dissect the contributions of the different EMF sources, Fig. 12(a) reports a set of pie charts over the measurement locations. The size of each chart is proportional to the total EMF strength of Fig. 11, while the shares of each chart are extracted from T1 of P4. Several considerations hold by analyzing Fig. 12(a). First, the contributions of 2G/3G/4G is

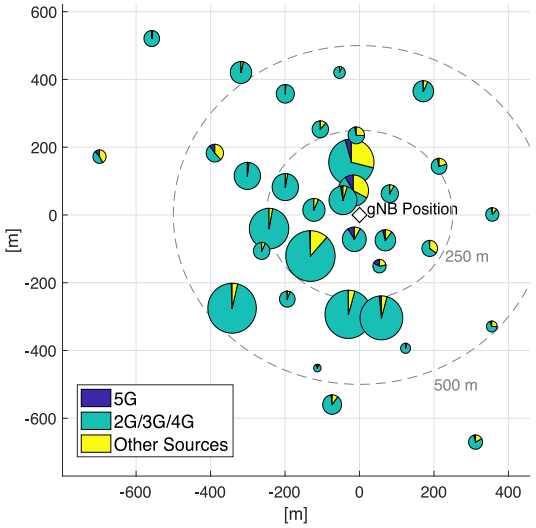

(a) Pie shares: PD extrapolated from T1 (5G, 2G/3G/4G, Other).

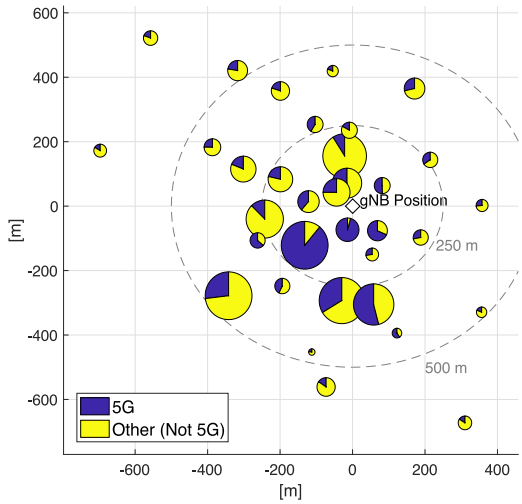

(b) Pie shares: PD extrapolated from T2 (5G) and from T4 (Total).

FIGURE 12. **Pie charts reporting the contribution of 5G w.r.t. other sources extrapolated with two different techniques (T1 + T4, T2 + T4). The size of each pie is proportional to the total EMF measured with the wide-band probe.**

always predominant w.r.t. 5G in all the locations. Moreover, a non-negligible amount of exposure is generated by other sources (which include, e.g., WiFi networks that are sensed outdoor). However, as reported by [15] the outcome of the max-hold analysis through a large span may be used only to detect the different technologies, and not to provide quantitative comparison. In fact, such measurements are retrieved over a large span - a setting that may severely impact the accuracy of the obtained results. To overcome such issues, Fig. 12(b) reports again the pie charts, by adopting in this case as pie shares the 5G exposure measured in RT (Fig. 10) and the exposure from other sources (computed as the root

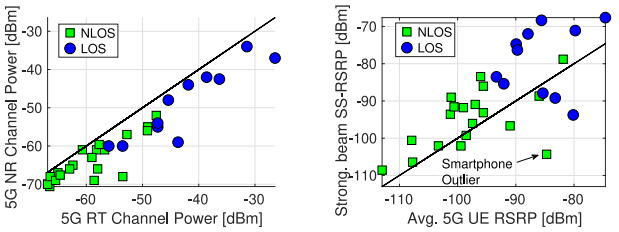

(a) 5G Channel Power vs. 5G RT Channel Power

(b) Strongest Beam SS-RSRP vs. 5G UE SS-RSRP

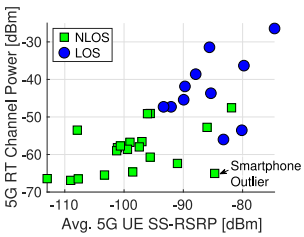

(c) 5G RT Channel Power vs. 5G UE SS-RSRP

FIGURE 13. **Comparison of channel power and SS-RSRP metrics for assessing the 5G exposure.**

square difference between the total EMF measured with the WB probe and the 5G RT EMF from the SA). This time, the contribution of 5G w.r.t. other (not 5G) sources becomes evident. In particular, 5G represents the largest exposure contribution in different points located in summits and canyons, typically in LOS and in proximity to the gNB (i.e., the locations on the center-to-bottom part of the figure). However, the share of 5G exposure w.r.t the total one is lower than 15% for the majority of the locations - a value lower than the one measured in South Korea by [32]. In addition, we point out that Italy is subject to stricter exposure limits than South Korea, thus resulting in (possibly) lower radiated power from 5G gNB and hence lower exposure levels. Moreover, another possibly explanation is that the analyzed 5G spectrum is equal to 20 [MHz], while other countries may adopt larger 5G spectrum (which may in turn require more power). Finally, the Italian operator may have opted to assign a large amount of the available power budget to pre-5G equipment rather than 5G one.

As a side comment, the measurement taken with the SA may be naturally different w.r.t. the one taken with the EMF meter, due to the following aspects: *i*) the EMF meter is in close proximity (but not exactly the same location) w.r.t. SA, *ii*) a directional probe is used with the SA, while the probe of the EMF meter is isotropic.

D. JOINT ANALYSIS AND OUTLIER DISCOVERY

During this part, we target the following question: is it possible to extract other useful information about 5G exposure, by jointly comparing the different metrics retrieved over the different steps in P4? To answer such question, Fig. 13 reports a comparison of: 5G New Radio (NR) channel power vs. 5G RT channel power (Fig. 13(a)), SS-RSRP of the strongest

beam vs. 5G UE SS-RSRP (Fig. 13(b)), and 5G RT channel power vs. 5G UE SS-RSRP. Several considerations hold by analyzing the figures. First, 5G NR channel power is proportional to 5G RT channel power (Fig. 13(a)). Obviously, the x-y values are not overlapping over the bisector line, due to the following reasons: *i*) 5G NR channel power is measured over a shorter time period w.r.t. 5G RT channel power, *ii*) 5G RT channel power may include the contributions from multiple sectors radiating over the same location, while 5G NR channel power is selective of the power received from the strongest sector. Interestingly, however, the highest values of channel power are recorded for both metrics in different locations lying in LOS conditions.

Moving then our attention to the comparison of strongest beam SS-RSRP vs. 5G UE SS-RSRP (Fig. 13(b)), the former is typically higher than the latter for most of locations. This behavior may be explained by the following reasons: *i*) adoption of different receiving antennas on the two measurement devices (SA vs. smartphone), *ii*) slightly different propagation conditions (we recall that we measure the SS-RSRP with the 5G UE in a radius of 10 [m] around the measurement location), and *iii*) averaging effect on the measurements collected with the 5th-generation cellular network (5G) UE. However, *i*) and *ii*) may actually result in lower SS-RSRP values collected with the SA w.r.t. the 5G UE (especially in LOS conditions). Moreover, the RSRP outlier that emerged in Fig. 6 is also evident in the bottom-right part of Fig. 13(b). In this location, in fact, the SS-RSRP measured with the SA was around -105 [dBm] (i.e., a very low value), while the same metric measured with the 5G UE was consistently higher. By further analyzing the output produced by CellMapper App, we have noticed that the smartphone reported RSRP values that were measured over 4G bands providing DSS functionality from the WindTre base station located on bottom right of Fig. 4, which was in LOS and almost at the same altitude w.r.t. the measurement location. However, such information was not saved on the CSV file saved by the application, which (wrongly) reported a large RSRP value over "pure" 5G frequencies. This fact further corroborates our intuition of adopting an integrated approach to cross-validate the measurements taken with different equipment tools.

Eventually, Fig. 13(c) reports a comparison between the total 5G RT channel power measured with the SA and the SS-RSRP measured with the 5G UE. Interestingly, we can note that the SS-RSRP is a good proxy for the RT channel power in many locations under LOS conditions. In particular, the higher is the value of SS-RSRP, the higher is also the value of measured RT channel power. Again, we can note that the smartphone outlier due to DSS can be easily grasped by observing the figure.

Finally, Table 3 reports the correlation coefficients and p-values for the metrics compared in Fig. 13 (by removing the aforementioned outlier). Clearly, the correlation of 5G NR channel power vs. 5G RT channel power is very high and largely significant (as expected). Moreover, a strong positive

TABLE 3. Correlation coefficients and p-values for different metrics.

Metric	Corr. Coefficient	p Value
5G NR channel power vs. 5G RT channel power	0.947	2.71×10^{-17}
strongest beam SS-RSRP vs. 5G UE SS-RSRP	0.760	1.2×10^{-6}
5G RT channel power vs. 5G UE SS-RSRP	0.758	1.72×10^{-6}

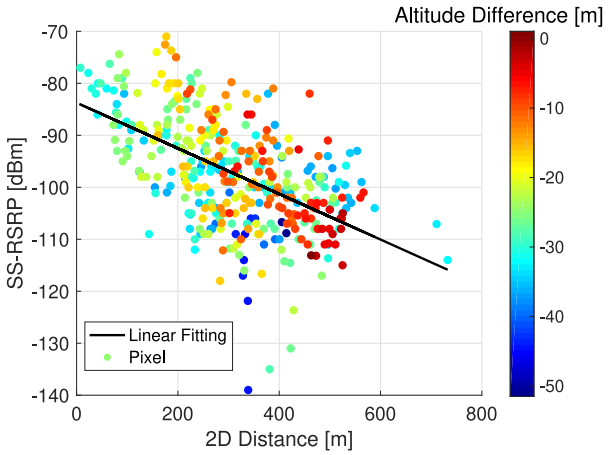

FIGURE 14. Smartphone 5G SS-RSRP (avg. values) vs. 2D distance from the 5G gNB. The point colors are proportional to the difference in altitude w.r.t. the 5G gNB (figure best viewed in colors).

(and significant) correlation is observed for the strongest beam SS-RSRP vs. 5G UE SS-RSRP and also for the 5G RT channel power vs. 5G UE SS-RSRP. This evidence substantiates the adoption of SS-RSRP measurement done with the 5G UE as a proxy for the 5G RT channel power measured with the SA.

E. DISTANCE-BASED ANALYSIS

In the following, we aim at shedding light about the impact of distance from the gNB on the measured exposure levels. To this aim, Fig. 14 reports the 5G UE SS-RSRP values vs. the 2D distance from the 5G UE. Each point represents a pixel in the territory. Moreover, the color is proportional to the difference in altitude $\delta_{(p,\mathrm{gNB})}$ between the measurement locations and the 5G panel. The figure reports also a simple linear fitting of the SS-RSRP values. Several considerations hold by analyzing the figure. First, the increase of distance tends to reduce the measured SS-RSRP values. This is an expected trend, due to the increase of the propagation loss. Second, $\delta_{(p,\mathrm{gNB})}$ plays a great role in further differentiating among the recorded SS-RSRP values - up to around 200 [m] from the gNB. In particular, the pixels experiencing the highest values of SS-RSRP are those ones were $|\delta_{(p,\mathrm{gNB})}| < 20$ [m], while lower SS-RSRP values are recorded for pixels subject to larger difference in altitude. However, when the distance from the gNB is increased, the impact of $\delta_{(p,\mathrm{gNB})}$ is less evident, possibly due to the fact that NLOS conditions dominate - leading to a prompt decrease of the observed SS-RSRP values.

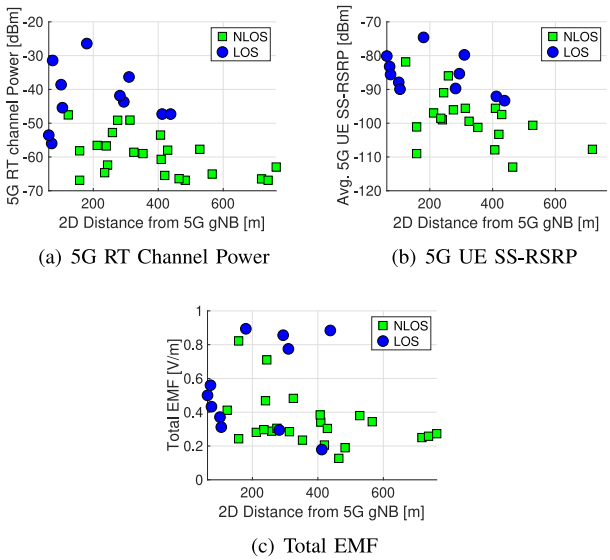

(a) 5G RT Channel Power (b) 5G UE SS-RSRP

(c) Total EMF

FIGURE 15. Comparison of 5G channel power, 5G SS-RSRP metrics and total EMF vs. distance.

TABLE 4. Correlation coefficients and p-values for different metrics vs. 2D distance.

Metric	Corr. Coefficient	p Value
5G RT channel power vs. 2D distance	-0.517	0.002
5G UE SS-RSRP vs. 2D distance	-0.576	8.61×10^{-4}
Total EMF vs. 2D distance	-0.329	0.058

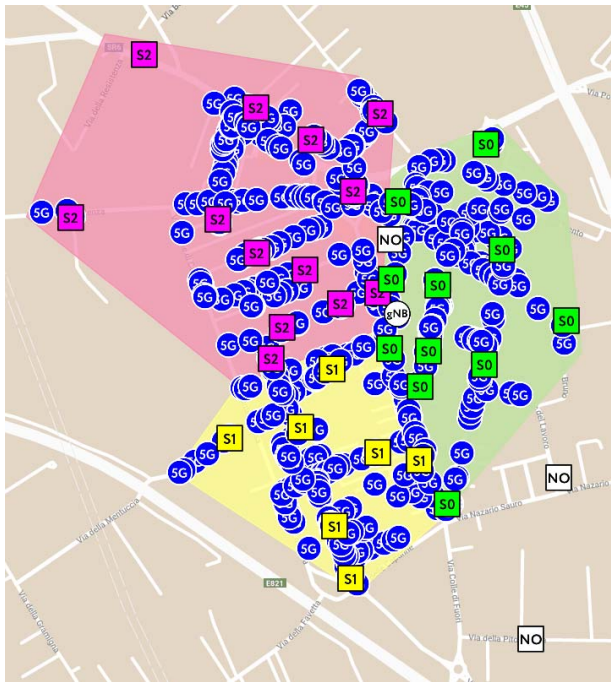

FIGURE 16. Smartphone 5G SS-RSRP measurements (5G blue pins), positioning of the 5G gNB (gNB white pin) and measurement points. The pin of each measurement point reports the sector ID: sector 0 ("S0" green pins), sector 1 ("S1" yellow pins), sector 2 ("S2" light red pins), sector ID not available ("NO" white pins) - figure best viewed in colors.

We then move our attention to the impact of distance over the metrics sensed in the measurement locations, as shown in Fig. 15. During this step, we select: 5G RT channel power, 5G UE SS-RSRP and total EMF. Moreover, Table 4 reports correlation coefficients and p-values for the aforementioned metrics vs. 2D distance from 5G gNB. Interestingly, similar trends are observed for the 5G RT channel power (Fig. 15(a)) and the 5G UE SS-RSRP (Fig. 15(b)). In particular, the increase of distance tends to reduce both the metrics. This fact is corroborated by Table 4, which reports negative correlation (and a significant outcome) for both metrics. Moreover, we can clear distinguish the LOS vs. NLOS locations in Fig. 15(a)–Fig. 15(b). Such considerations do not apply to the total EMF vs. distance, shown in Fig. 15(c). In this case, there is not a clear decreasing trend vs. distance, and the different sight conditions do not substantially affect the metric. Therefore, the correlation of the total EMF vs. distance reported in Table 4 appears to be rather modest (and not significant). Obviously, the presence of other EMF sources different than 5G (including the other pre-5G base station in the town) strongly impacts the total EMF that is measured in each location, thus confirming that the best way to capture the 5G exposure is to perform selective measurements (first with 5G UE and then with SA).

F. SECTOR-BASED ANALYSIS

In the final part of our work, we integrate the cell ID measured during T3 of P4 with the other measurements. Fig. 16 reports the characterization of SS-RSRP for each sector. The size of each sector almost corresponds to the locations where the same sector ID has been sensed. In addition, different measurement locations were added on purpose in order to distinguish the border of each sector. Clearly, when multiple sectors radiate over the same location (due to a slight overlapping), we assign the location to the sector with the highest measured SS-RSRP value. Interestingly, the considered 5G gNB implements a typical three-sectorization, in which the extent of sector S2 appears to be consistently higher than the other sectors. Moreover, the horizontal width of S0 is clearly wider than S1 and S2. In addition, we were able to decode the 5G signal for the location on top-left of the figure, in which no 5G coverage was measured with the smartphone, while the SA was able to perform the 5G measurements. On the other hand, we did not find any 5G coverage (even with the SA) for the two locations located on bottom right of Fig. 16. As a side comment, we also find a coverage hole close to the gNB (center-to-top of the figure). Such location was subject to NLOS conditions, lying on the border of two different sectors (S0 and S2).

After assigning each pixel to a given sector, we have analyzed the differences/similarities over the metrics for each sector. Fig. 17(a) reports the Empirical Cumulative Distribution Function (ECDF) of the 5G UE SS-RSRP values over the three sectors. Interestingly, the SS-RSRP values from S2 and S1 are lower than S0. By further investigating this issue, we have found that the observed 3D distance is clearly lower in S0 w.r.t. S1 and S2 - a condition that

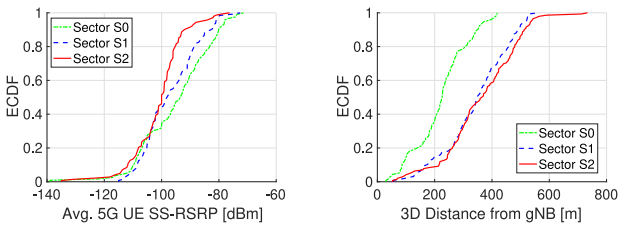

(a) 5G SS-RSRP (b) 3D Distance

FIGURE 17. Sector-based Empirical Cumulative Distribution Functions (ECDFs) of the 5G SS-RSRP measured with the smartphone and the 3D distance from the 5G gNB.

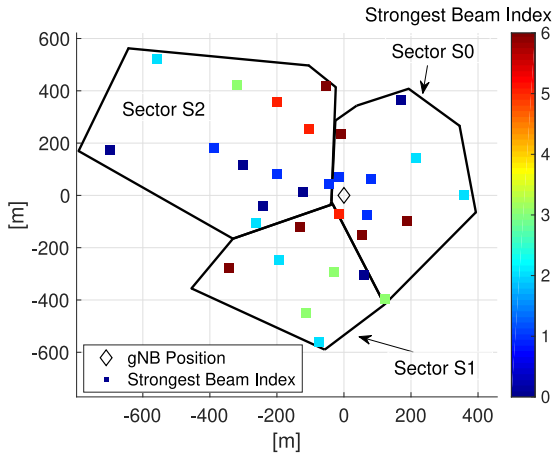

FIGURE 18. Index of the strongest beam for the SSB measured with the 5G NR module of the SA (figure best viewed in colors).

generally results in worser propagation conditions and thus (possibly) explaining the difference in the observed SS-RSRP values.

In the next part, we report the sector-based analysis of the strongest beam index, shown in Fig. 18. Interestingly, the strongest beam tends to notably vary over the measurement locations. Clearly, this metric depends on the actual positioning of the control beams over the territory. Nevertheless, we observed similar cardinalities in terms of total number of deployed beams - up to 6 for each sector.

We then move our attention to the relative difference between the 5G NR channel power and the 5G RT channel power, shown in Fig. 19. Interestingly, the difference of channel power is extremely low for the LOS locations of S0 w.r.t. to S1 and S2. On the other hand, large difference of channel power are experienced in different locations of S1 and S2. Such deviations may be explained by a slight overlapping of S0 and S2 in the zone covered by S1. However, other effects may impact the observed channel power difference in S2, which include, e.g., slightly different propagation conditions and/or different traffic patterns that are experienced during T2 and T3.

In the last part of our work, we exploit the information about the extent of the sectors to estimate the power radiated by each panel. Initially, we select the locations for each sector by observing the 5G UE SS-RSRP over the territory, as

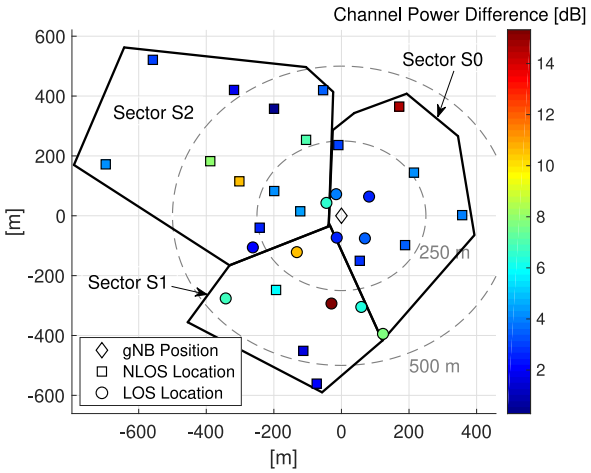

FIGURE 19. Difference between 5G RT channel power and 5G NR channel power in each measurement spot, with sectorization detail.

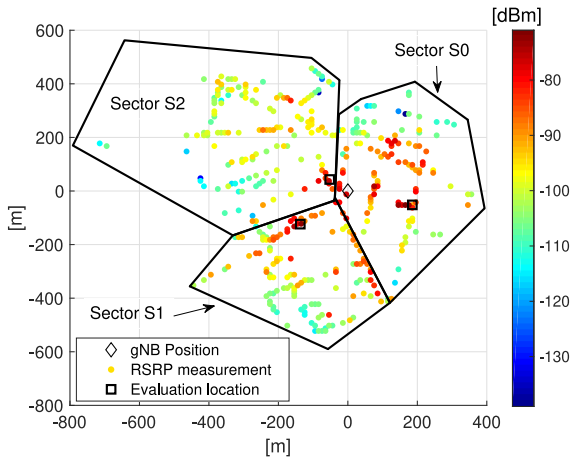

FIGURE 20. Positioning of the locations to evaluate the 5G transmitted power.

reported in Fig. 20. In particular, we select three representative locations, subject to LOS conditions and large SS-RSRP values - marked with squares in the figure. In the following step, we perform a long recording of the 5G RT channel power over a period of 15 [m] in each evaluation location. Fig. 21 and Fig. 22 report the recorded spectrogram and the average 5G spectrum, respectively. By analyzing such figures, we can clearly see that the 5G spectrum is effectively exploited to carry traffic generated by other UE in the territory (not under our control), as the observed trend is completely different w.r.t. one recorded in other locations not subject to high traffic conditions (see, e.g., Fig. 2).[17] However, the spectrograms reported in Fig. 21 reveal that S0 substantially differs w.r.t. S1 and S2. For this location, in fact, the observed 5G spectrum is not always constant over time. Since the oscillations in the received power are experienced over the whole 5G spectrum (and not only on

17. We notice that the operator has imposed a resource allocation policy to prioritize the usage of the 5G spectrum up to around 3618 [MHz], while leaving the additional BW (up to the guard band) almost empty.

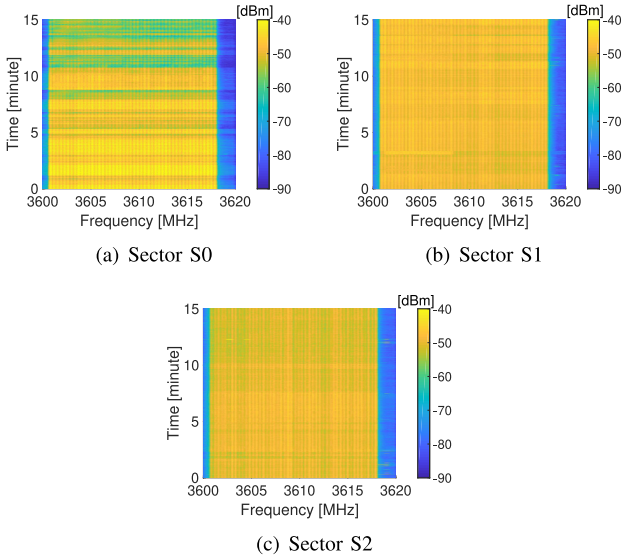

(a) Sector S0 (b) Sector S1

(c) Sector S2

FIGURE 21. 5G RT spectrograms over the evaluation locations (subfigures best viewed in colors).

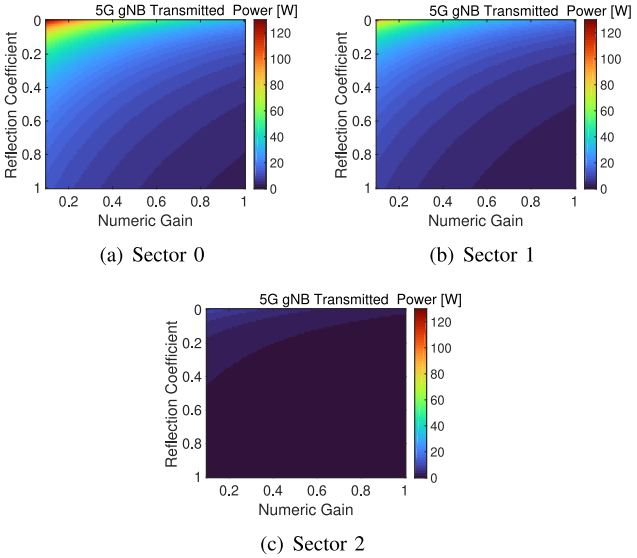

(a) Sector 0 (b) Sector 1

(c) Sector 2

FIGURE 23. Estimated transmitted power for each sector vs. numeric gain and reflection coefficients variations (subfigures best viewed in colors).

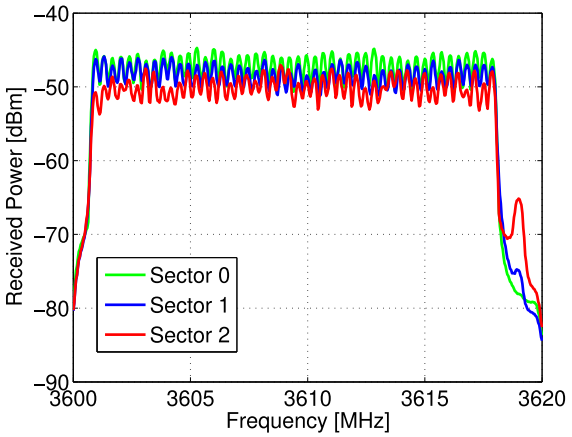

FIGURE 22. Average 5G spectrum in the evaluation locations.

selected portions), we argue that such behavior may be due to a slight change in the reflection conditions experienced during the measurement. In the following step, we compute the total PD power density Λ_{5G} by applying Eq. (3) over the recorded values of $\sigma_{(f,t)}$ (shown in Fig. 21). Given the total PD in each location, we adopt the point-source model of ITU [10], [11] to estimate the total radiated power P_{5G} as:

$$P_{5G} = \frac{\Lambda_{5G} \cdot 4\pi \cdot \delta^2_{(p,\text{gNB})}}{G^{\text{TX}} \cdot H \cdot (1+\Gamma)^2} \tag{9}$$

where: $\delta_{(p,\text{gNB})}$ is the 3D-distance between the pixel p of the location and the gNB, G^{TX} is the transmission gain (i.e., the maximum gain of the transmitting antenna, relative to an isotropic radiator), H is the antenna numeric gain (a.k.a. antenna pattern) and Γ is the reflection coefficient [33]. To evaluate P_{5G}, we consider $G^{\text{TX}} = 15$ [dB] [11], $\Gamma \in [0, 1]$, corresponding to the full range between no reflection ($\Gamma = 0$) up to a complete reflection ($\Gamma = 1$). Focusing on H, the numeric gain parameters are (obviously) not available. To overcome such issue, we have considered a wide range for H, up to the maximum value of 1 [11]. Consequently, Fig. 23 reports the estimated value of P_{5G} for the different sectors vs. antenna numeric gain and reflection coefficients. Interestingly, the power radiated by each sector is at most equal to 130 [W] - a value consistently lower than the maximum equipment power (set to 200 [W] for similar panels from other vendors [34]). Moreover, several differences emerge when comparing the outcomes from the different sectors. In particular, the radiated power from S2 appears to be significantly lower than the one from S0 and S1. This outcome may be explained by the presence of buildings in close proximity to sector S2, which may impact the maximum exposure of the sector allowed by regulations. Alternatively, another explanation may be that setting of the electrical tilting is different w.r.t. the other two sectors, thus resulting in a radiation pattern not completely oriented towards the evaluation location for S2 (which we remind is placed at a closer distance w.r.t. the other evaluation spots).

V. CONCLUSION AND FUTURE WORK

We have tackled the problem of massively measuring the 5G exposure in a town, by proposing and evaluating an integrated approach. To this aim, we exploit the SS-RSRP measured with the 5G smartphone to tune the selection of locations for performing comprehensive measurements with the SA and the EMF meter. Results, obtained over a realistic scenario, actually provide interesting insights about 5G exposure. First of all, our work indicates that the 5G SS-RSRP measured with the smartphone is a good indicator of the 5G RT channel power. However, the 5G UE SS-RSRP has to be carefully integrated with the detailed exposure metrics retrieved from the SA, in order to locate and explain outliers due, e.g., to DSS. In addition, our work indicates that the

exposure from 5G gNB is overall lower than 0.7 [V/m] - and typically representing a small share compared to other sources. Moreover, we have demonstrated that the propagation conditions (LOS vs. NLOS, distance from the gNB) play a great role in determining the level of exposure from 5G gNB. Eventually, we have studied the features of each sector, showing that multiple control beams are deployed over the territory and that a slight overlap among the sectors emerges. Finally, we have estimated the power radiated by each sector, finding that this metric is typically lower than the maximum one.

We believe that this work can be a first step towards a more comprehensive approach. First of all, given that the 5G NR channel power is highly correlated with the 5G RT channel power, we plan to further revise our approach to further decrease the measurement time spent in each location. For example, an interesting step could be to solely measure the 5G NR channel power in the selected locations, while leaving the evaluation of 5G RT channel power only to a limited subset of locations. Second, the integration of 5G scanners, as well as fixed 5G sensors, is an interesting avenue of further research. Eventually, we plan to extend our work to the off-peak hours (in order to study possible deviations w.r.t. the peak values measured in this work). Third, the evaluation of exposure in the uplink and downlink direction over the different measurement locations is another interesting research direction. Finally, we plan to repeat our measurements under heavy traffic conditions, in order to check whether the good level of correlation shown between the 5G RT channel power and the 5G UE SS-RSRP is confirmed also in this case.

APPENDIX A
ACRONYMS LIST

Table 5 reports the list of acronyms used in our work.

TABLE 5. List of Acronyms.

Acronym	Definition
BW	BandWidth
DEI	Digital Elevation Information
DSS	Dynamic Spectrum Sharing
ECDF	Empirical Cumulative Distribution Function
EMF	ElectroMagnetic Field
GPS	Global Positioning System
HW	HardWare
IEC	International Electrotechnical Commission
ITU	International Telecommunication Union
gNB	next-generation Node-B
LOS	Line-of-Sight
NB	NarrowBand
NBW	Equivalent Noise Bandwidth
NLOS	Non-Line-of-Sight
NR	New Radio
PBCH	Physical Broadcast CHannel
PD	Power Density
QPSK	Quadrature Phase Shift Keying
RBW	Resolution BandWidth
RSRP	Reference Signal Received Power
RT	Real Time
RTSA	Real Time Spectrum Analysis
SA	Spectrum Analyzer
SCS	SubCarrier Spacing
SIM	Subscriber Identity Module
SSB	Synchronization Signal Block
SS-RSRP	Synchronization Signals - Reference Signal Received Power
UE	User Equipment
VBW	Video BandWidth
WB	Wide Band
5G	5th-generation cellular network

APPENDIX B
TOTAL PD EXTRAPOLATION

In this Appendix, we provide more details on how the total PD Λ_{5G} has been extrapolated from the measured samples $\rho_{(f,t_{END})}$. We start from the 5G channel power computation of [8]:

$$C_{5G\text{-}SWP} = \frac{B_{5G}}{\kappa \cdot RBW} \frac{1}{N_{SAM}} \sum_{f \in \mathcal{F}_{5G}} \sigma_{(f,t_{END})} \quad [W] \quad (10)$$

where $C_{5G\text{-}SWP}$ is the 5G channel power over a single sweep, B_{5G} is the bandwidth of the 5G channel, RBW is the resolution bandwidth of the SA, κ is an SA corrective parameter to compute the equivalent noise bandwidth NBW $= \kappa \cdot$RBW from the resolution bandwidth, N_{SAM} is the number of samples over the single sweep, $\mathcal{F}_{5G}$ is the set of 5G frequencies over the considered sweep, and $\sigma_{(f,t_{END})}$ is the measured received power over frequency $f \in \mathcal{F}_{5G}$ and the final time slot t_{END}.

By considering in more detail Eq. (10), we can note that the channel power (i.e., the total power in the considered frequency range) is derived by: *i*) averaging the received power over the considered samples, *ii*) normalizing the average received power by $\kappa \cdot$ RBW [Hz], in order to get the average power per Hertz, *iii*) rescaling the term in *ii*) by B_{5G} to obtain the total average received power over the whole 5G channel.

When providing the PD term $\rho_{(f,t_{END})}$, the SA simply applies the following (trivial) equation:

$$\rho_{(f,t_{END})} = \frac{\sigma_{(f,t_{END})}}{A_f} \quad \left[W/m^2\right] \quad (11)$$

where A_f is the antenna efficiency, which is computed by the SA given as input the values of antenna factor of the received antenna that were loaded on the SA. Therefore, in order to get the total PD Λ_{5G}, we need to apply the same operations performed in Eq. (10), namely: *i*) average PD computation, *ii*) $\kappa \cdot$ RBW normalization, *iii*) B_{5G} scaling. More formally, Λ_{5G} is given by:

$$\Lambda_{5G} = \frac{B_{5G}}{\kappa \cdot RBW} \frac{1}{N_{SAM}} \sum_{f \in \mathcal{F}_{5G}} \rho_{(f,t_{END})} \quad \left[W/m^2\right] \quad (12)$$

The total 5G BW B_{5G} can be alternatively expressed as:

$$B_{5G} = \Delta_f \times N_{SAM} \quad [Hz] \quad (13)$$

where we remind that Δ_f is the frequency spacing between two consecutive samples of the SA.

By replacing the B_{5G} term of Eq. (13) in Eq. (12) we finally get:

$$\Lambda_{5G} = \frac{1}{\kappa \cdot RBW} \sum_{f \in \mathcal{F}_{5G}} \rho_{(f,t_{END})} \cdot \Delta_f \quad \left[W/m^2\right]. \quad (14)$$

REFERENCES

[1] M. Simkó and M.-O. Mattsson, "5G wireless communication and health effects: A pragmatic review based on available studies regarding 6 to 100 GHz," *Int. J. Environ. Res. Public Health*, vol. 16, no. 18, p. 3406, 2019.

[2] L. Chiaraviglio, A. Elzanaty, and M.-S. Alouini, "Health risks associated with 5G exposure: A view from the communications engineering perspective," *IEEE Open J. Commun. Soc.*, early access. [Online]. Available: https://ieeexplore.ieee.org/document/9518367/

[3] L. Chiaraviglio, M. Fiore, and E. Rossi, "5G technology: Which risks from the health perspective," in *The 5G Italy Book*. Parma, Italy: CNIT, 2019.

[4] D. Colombi *et al.*, "Assessment of actual maximum RF EMF exposure from radio base stations with massive MIMO antennas," in *Proc. Photon. Electromagn. Res. Symp. Spring (PIERS-Spring)*, 2019, pp. 570–577.

[5] B. Thors, D. Colombi, Z. Ying, T. Bolin, and C. Törnevik, "Exposure to RF EMF from array antennas in 5G mobile communication equipment," *IEEE Access*, vol. 4, pp. 7469–7478, 2016.

[6] *3GPP Dynamic Spectrum Sharing*. Accessed: Jun. 30, 2021. [Online]. Available: https://www.3gpp.org/dss

[7] L. Chiaraviglio *et al.*, "Planning 5G networks under EMF constraints: State of the art and vision," *IEEE Access*, vol. 6, pp. 51021–51037, 2018.

[8] *CEI 211-7/E Guida Per La Misura e Per La Valutazione Dei Campi Elettromagnetici Nell'intervallo Di Frequenza 10 kHz–300 GHz, Con Riferimento All'esposizione Umana appendice E: Misura Del Campo Elettromagnetico Da Stazioni Radio Base Per Sistemi Di Comunicazione Mobile (2G, 3G, 4G, 5G)*. Accessed: Jun. 15, 2021. [Online]. Available: https://mycatalogo.ceinorme.it/cei/item/0000017160?lang=en

[9] *Field Master Pro MS2090A Specifications*. Accessed: Jun. 30, 2021. [Online]. Available: https://www.anritsu.com/en-us/test-measurement/products/ms2090a

[10] *ITU-T K.52 : Guidance on Complying With Limits for Human Exposure to Electromagnetic Fields*. Accessed: Jul. 25, 2018. [Online]. Available: https://www.itu.int/rec/T-REC-K.52/en

[11] *ITU-T K70 Mitigation Techniques to Limit Human Exposure to EMFs in the Vicinity of Radiocommunication Station*. Accessed: Oct. 25, 2020. [Online]. Available: https://www.itu.int/rec/T-REC-K.70/en

[12] *IEC 62232:2017 Determination of RF Field Strength, Power Density and SAR in the Vicinity of Radiocommunication Base Stations for TH Epurpose of Evaluating Human Exposure*. Accessed: Feb. 27, 2020. [Online]. Available: https://webstore.iec.ch/publication/62014

[13] *IEC 62669:2019 Case Studies Supporting IEC 62232—Determination of RF Field Strength, Power Density and SAR in the Vicinity of Radiocommunication Base Stations for the Purpose of Evaluating Human Exposure*. Accessed: Feb. 27, 2020. [Online]. Available: https://webstore.iec.ch/publication/62014

[14] *TESTO COORDINATO DEL DECRETO-LEGGE 18 Ottobre 2012, n. 179 Ulteriori Misure Urgenti Per La Crescita Del Paese.* Accessed: Jan. 29, 2018. [Online]. Available: www.gazzettaufficiale.it/eli/id/2012/12/18/12A13277/sg

[15] S. Aerts *et al.*, "*In-situ* measurement methodology for the assessment of 5G NR massive MIMO base station exposure at sub-6 GHz frequencies," *IEEE Access*, vol. 7, pp. 184658–184667, 2019.

[16] S. Aerts *et al.*, "*In Situ* assessment of 5G NR massive MIMO base station exposure in a commercial network in bern, switzerland," *Appl. Sci.*, vol. 11, no. 8, p. 3592, 2021.

[17] D. Franci *et al.*, "Experimental procedure for fifth generation (5G) electromagnetic field (EMF) measurement and maximum power extrapolation for human exposure assessment," *Environments*, vol. 7, no. 3, p. 22, 2020.

[18] S. Adda *et al.*, "A theoretical and experimental investigation on the measurement of the electromagnetic field level radiated by 5G base stations," *IEEE Access*, vol. 8, pp. 101448–101463, 2020.

[19] C. Bornkessel, T. Kopacz, A.-M. Schiffarth, D. Heberling, and M. A. Hein, "Determination of instantaneous and maximal human exposure to 5G massive-MIMO base stations," in *Proc. 15th Eur. Conf. Antennas Propag. (EuCAP)*, 2021, pp. 1–5.

[20] D. Colombi, P. Joshi, B. Xu, F. Ghasemifard, V. Narasaraju, and C. Törnevik, "Analysis of the actual power and EMF exposure from base stations in a commercial 5G network," *Appl. Sci.*, vol. 10, no. 15, p. 5280, 2020.

[21] A.-K. Lee, S.-B. Jeon, and H.-D. Choi, "EMF levels in 5G new radio environment in Seoul, Korea," *IEEE Access*, vol. 9, pp. 19716–19722, 2021.

[22] C. Carciofi, A. Garzia, S. Valbonesi, A. Gandolfo, and R. Franchelli, "RF electromagnetic field levels extensive geographical monitoring in 5G scenarios: Dynamic and standard measurements comparison," in *Proc. IEEE Int. Conf. Technol. Entrepreneurship (ICTE)*, 2020, pp. 1–6.

[23] *Rohde and Schwarz TSMA6 Autonomous Mobile Network Scanner User Manual*. Accessed: Jun. 16, 2021. [Online]. Available: https://tinyurl.com/5bjbffpz

[24] *Antenna Factor Diagram HyperLOG 6080 Datasheet*. Accessed: Jun. 24, 2021. [Online]. Available: https://aaronia-shop.com/products/logper-antenna-hyperlog6080

[25] *WaveControl WPF8 Field Probe Datasheet*. Accessed: Oct. 29, 2019. [Online]. Available: https://www.wavecontrol.com/rfsafety/images/data-sheets/en/WPF8_Datasheet_EN.pdf

[26] *WaveControl WPF8 Probe*. Accessed: Jun. 16, 2021. [Online]. Available: https://www.wavecontrol.com/rfsafety/images/data-sheets/en/WPF8_Datasheet_EN.pdf

[27] *WaveControl WPFT Probe*. Accessed: Jun. 16, 2021. [Online]. Available: https://www.wavecontrol.com/rfsafety/en/products/probes

[28] S. Tarquini and L. Nannipieri, "The 10 m-resolution TINITALY DEM as a trans-disciplinary basis for the analysis of the Italian territory: Current trends and new perspectives," *Geomorphology*, vol. 281, pp. 108–115, Mar. 2017.

[29] L. Chiaraviglio, J. Galán-Jiménez, M. Fiore, and N. Blefari-Melazzi, "Not in my neighborhood: A user equipment perspective of cellular planning under restrictive EMF limits," *IEEE Access*, vol. 7, pp. 6161–6185, 2018.

[30] *Agilent Spectrum Analyzer Measurements and Noise Application Note 1303*. Accessed: Jun. 24, 2021. [Online]. Available: http://www.av.it.pt/medidas/Data/Manuais

[31] *5G NR Code Selective EMF Measurements*. Accessed: Jun. 24, 2021. [Online]. Available: https://www.itu.int/en/ITU-D/Regional-Presence/Europe/Documents/Events/2020/Spectrum_EUR_CIS/Manuel

[32] B. Selmaoui, P. Mazet, P.-B. Petit, K. Kim, D. Choi, and R. de Seze, "Exposure of South Korean population to 5G mobile phone networks (3.4–3.8 GHz)," *Bioelectromagnetics*, vol. 42, no. 5, pp. 407–414, 2021.

[33] O. Landron, M. J. Feuerstein, and T. S. Rappaport, "A comparison of theoretical and empirical reflection coefficients for typical exterior wall surfaces in a mobile radio environment," *IEEE Trans. Antennas Propag.*, vol. 44, no. 3, pp. 341–351, Mar. 1996.

[34] *Antenna Integrated Radio Unit Description—Ericsson*. Accessed: Jul. 28, 2020. [Online]. Available: http://www.1com.net/wp-content/uploads/2019/09/sales@1com.com-Ericsson-AIR-6488-Integrated-Radio-Unit-Datasheet.pdf

LUCA CHIARAVIGLIO (Senior Member, IEEE) received the Ph.D. degree in telecommunication and electronics engineering from the Politecnico di Torino, Italy. He is an Associate Professor with the University of Rome Tor Vergata, Italy, and a Research Associate with CNIT, Italy. He has coauthored more than 140 papers published in international journals, books and conferences. His current research topics cover 5G networks, optimization applied to telecommunication networks, and health risks assessment of 5G communications. He has received the Best Paper Award at IEEE VTC-Spring 2020, IEEE VTC-Spring 2016, and ICIN 2018 all of them appearing as first author. Some of his papers are listed as Best Readings on Green Communications by IEEE. Moreover, he has been recognized as an author in the top 1% most Highly Cited papers in the ICT field worldwide. He is a TPC member of IEEE INFOCOM, an Associate Editor for *IEEE Communications Magazine* and IEEE TRANSACTIONS ON GREEN COMMUNICATIONS AND NETWORKING, and a Specialty Chief Editor of *Frontiers in Communications and Networks*.

CHIARA LODOVISI received the Ph.D. degree in engineering electronics from the University of Rome Tor Vergata, Italy. He is a Researcher with CNIT, Italy, and also with the University of Rome Tor Vergata. She worked for five years as an RF Engineer Consultant for H3G mobile operator. For five years, she worked on optical communications, study and implementation of submarine and satellite optical links and radio over fiber. Her research topics concern 5G networks, health risk assessment of 5G communications, interoperability over fiber between TETRA/LTE systems, and 5G networks.

DANIELE FRANCI received the M.Sc. degree *(cum laude)* and the Ph.D. degree in nuclear and subnuclear physics from the Sapienza University of Rome, Rome, Italy, in 2007 and 2011, respectively. From 2009 to 2011, he was a Technology Analyst with Nucleco S.p.A, involved in the radiological characterization of radioactive wastes from the decommissioning of former Italian nuclear power plants. He joined Agenzia per la Protezione Ambientale del Lazio in 2011, being involved in RF-EMF human exposure assessment. Since 2017, he has been involved in the activities with the Italian Electro Technical Committee for the definition of technical procedures for EMF measurement from 4G/5G mMIMO sources.

SETTIMIO PAVONCELLO was born in Rome, Italy, in 1973. He received the M.Sc. degree in telecommunications engineering from the Sapienza University of Rome, Rome, in 2001. Since 2002, he has been working with the EMF Department, Agenzia per la Protezione Ambientale del Lazio, Rome. He is specialized in electromagnetic field measurements and EMF projects evaluation related to radios, TVs, and mobile communications systems maturing huge experience in the use of broadband and selective instruments. In past years, he has deepened in the issues related to measurements on LTE and NB-IoT signals. Since 2018, he has been actively involved in the working group of the Italian Electrotechnical Committee aimed at defining measurement procedures for mobile communications signals and is currently engaged in various projects concerning measurement on 5G signals.

TOMMASO AURELI received the M.Sc. degree in biological science from the Sapienza University of Rome, Rome, Italy, in 1985. He joined Agenzia per la Protezione Ambientale del Lazio (ARPA Lazio) in 2002. From 2004 to 2018, he was the Director of EMF Division, being involved in both measurement and provisional evaluation EMF from civil sources. He is currently the Director of the Department of Rome, ARPA Lazio.

NICOLA BLEFARI-MELAZZI is currently a Full Professor of Telecommunications with the University of Rome "Tor Vergata", Italy. He is currently the Director of CNIT, a consortium of 37 Italian Universities. He has participated in over 30 international projects, and has been the principal investigator of several EU funded projects. He has been an Evaluator for many research proposals and a Reviewer for numerous EU projects. He has authored/coauthored about 200 articles, in international journals and conference proceedings. His research interests include the performance evaluation, design and control of broadband integrated networks, wireless LANs, satellite networks, and of the Internet.

MOHAMED-SLIM ALOUINI (Fellow, IEEE) was born in Tunis, Tunisia. He received the Ph.D. degree in electrical engineering from the California Institute of Technology, Pasadena, CA, USA, in 1998. He served as a Faculty Member of the University of Minnesota, Minneapolis, MN, USA, then with Texas A&M University at Qatar, Education City, Doha, Qatar before joining the King Abdullah University of Science and Technology, Thuwal, Makkah Province, Saudi Arabia, as a Professor of Electrical Engineering in 2009. His current research interests include modeling, design, and performance analysis of wireless communication systems.